Intrathymic adeno-associated virus gene transfer rapidly restores thymic function and long-term persistence of gene-corrected T cells

Marie Pouzolles, Alice Machado, Mickaël Guilbaud, Magali Irla, Sarah Gailhac, Pierre Barennes, Daniela Cesana, Andrea Calabria, Fabrizio Benedicenti, Arnauld Sergé, et al.

Intrathymic AAV gene transfer rapidly restores thymic function and long-term persistence of gene-corrected T cells

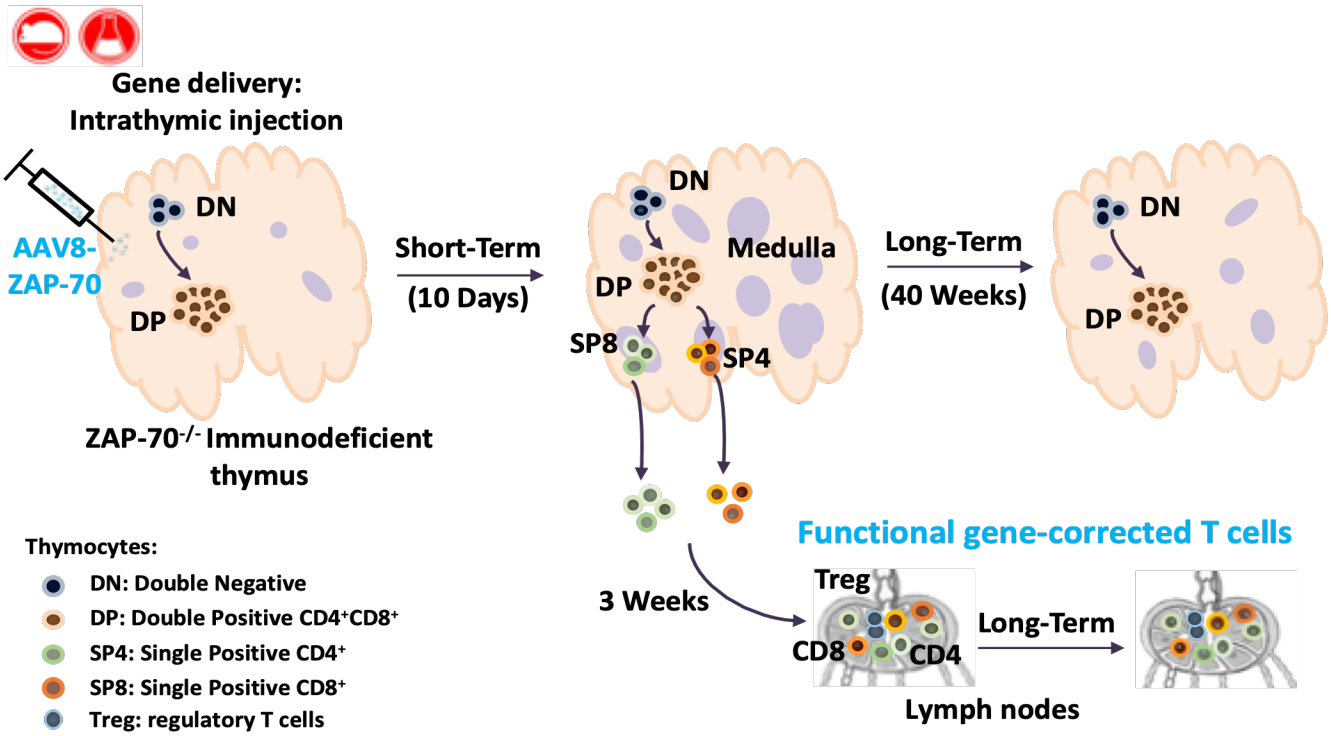

Intrathymic AAV gene transfer rapidly restores thymic function and long-term persistence of gene-corrected T cells

Marie Pouzolles, PhD[1]; Alice Machado, MSc[1#]; Mickaël Guilbaud, MSc[2#]; Magali Irla, PhD[3]; Sarah Gailhac, MSc[1]; Pierre Barennes, MSc[4]; Daniela Cesana, PhD[5]; Andrea Calabria, PhD[5]; Fabrizio Benedicenti, PhD[5]; Arnauld Sergé, PhD[3], Indu Raman, MSc[6]; Quan-Zhen Li, MD, PhD[6,7], Eugenio Montini, PhD[5]; David Klatzmann, MD, PhD[4,8], Oumeya Adjali, MD, PhD[2*]; Naomi Taylor, MD, PhD[1,9*]; and Valérie S. Zimmermann, PhD[1*]

[1]Institut de Génétique Moléculaire de Montpellier, University of Montpellier, CNRS, Montpellier, France; [2]INSERM UMR1089, Université de Nantes, Centre Hospitalier Universitaire de Nantes, Nantes, France; [3]Center of Immunology Marseille-Luminy (CIML), INSERM U1104, CNRS UMR7280, Aix-Marseille Université UM2, Marseille, 13288 cedex 09, France; [4]Sorbonne Université, INSERM, Immunology-Immunopathology-Immunotherapy (i3), Paris, France; [5]San Raffaele Telethon Institute for Gene Therapy (SR-Tiget), IRCCS, San Raffaele Scientific Institute, Milan, 20132, Italy; [6]Microarray Core Facility, University of Texas Southwestern Medical Center, Dallas, TX, USA ; [7]Department of Immunology, University of Texas Southwestern Medical Center, Dallas, TX, USA; [8]AP-HP, Hôpital Pitié-Salpêtrière, Biotherapy (CIC-BTi) and Inflammation-Immunopathology-Biotherapy Department (i2B), Paris, France; [9]Present address: Pediatric Oncology Branch, Center for Cancer Research, National Cancer Institute, National Institutes of Health (NIH), Bethesda, Maryland

[#]equal contribution

*Co-corresponding authors: O. Adjali, N. Taylor or V.S. Zimmermann, Institut de Génétique Moléculaire de Montpellier, 1919 Route de Mende, 34293 Montpellier, Cedex 5, France; Tel: 33 4 67 61 36 29, Fax: 33 4 67 04 02 31; emails: oumeya.adjali@univ-nantes.fr, taylorn4@mail.nih.gov, zimmermann@igmm.cnrs.fr

Funding Sources: M.P. was supported by a PhD fellowship from the LABEX EpiGenMed and the FRM. M.I. and O.A. are supported by INSERM, N.T. by INSERM and the NIH, and V.Z. by CNRS. This work was funded by the AFM, grant R01AI059349 from the National Institute of Allergy and Infectious Diseases, the ANR, ARC and INCa.

Disclosure statement: None of the authors have any disclosures to declare.

ABSTRACT

Background: Patients with T cell immunodeficiencies are generally treated by allogeneic hematopoietic stem cell transplantation but alternatives are needed for patients without matched donors. An innovative intrathymic (IT) gene therapy approach, directly targeting the thymus, may improve outcome.

Objective: To determine the efficacy of IT-adeno-associated virus (AAV) serotypes to transduce thymocyte subsets and correct the T cell immunodeficiency in a ZAP-70-deficient murine model.

Methods: AAV serotypes were injected intrathymically into WT mice and gene transfer efficiency was monitored. ZAP-70$^{-/-}$ mice were intrathymically injected with an AAV8 vector harboring the ZAP-70 gene. Thymus structure, immunophenotyping, TCR clonotypes, T cell function, immune responses to transgenes and autoantibodies, vector copy number and integration were evaluated.

Results: AAV 8, 9 and 10 serotypes all transduced thymocyte subsets following *in situ* gene transfer, with transduction of up to 5% of cells. IT injection of an AAV8-ZAP-70 vector into ZAP-70$^{-/-}$ mice resulted in a rapid thymocyte differentiation, associated with the development of a thymic medulla. Strikingly, medullary thymic epithelial cells expressing the autoimmune regulator AIRE were detected within 10 days of gene transfer, correlating with the presence of functional effector and regulatory T cell subsets with diverse TCR clonotypes in the periphery. While thymocyte reconstitution was transient, gene-corrected peripheral T cells, harboring approximately 1 AAV genome/ cell, persisted for >40 weeks and AAV vector integration was detected.

Conclusions: Intrathymic AAV-transduced progenitors promote a rapid restoration of the thymus architecture with a single wave of thymopoiesis generating long-term peripheral T cell function.

Key Messages:

- Intrathymic AAV gene correction of an immunodeficiency promotes the differentiation of a normal thymic architecture within 10 days post gene transfer
- Intrathymic AAV gene transfer results in vector integration with the persistence of gene-corrected peripheral T cells for >40 weeks

Capsule Summary:

Intrathymic AAV-mediated gene therapy presents a novel therapeutic option for immunodeficient patients, promoting a rapid reconstitution of the thymic environment and subsequent T cell reconstitution.

Key Words:

Severe combined immunodeficiency, Gene therapy, ZAP-70, thymus, intrathymic gene transfer, medulla formation, T cell reconstitution, humoral immunity

Abbreviations:

AAV: adeno-associated virus

AIRE: autoimmune regulator

DN: double negative CD4-CD8-

DP: double positive CD4+CD8+

ELISA: enzyme-linked immunosorbent assay

GvHD: graft versus host disease

HLA: human leukocyte antigen

HSC: hematopoietic stem cell

Ig: immunoglobulin

IT: intrathymic

IV: intravenous

LN: lymph node

MFI: mean fluorescence intensity

mTEC: medullary thymic epithelial cell

PCR: polymerase chain reaction

PID: primary immunodeficiency

SCID: severe combined immunodeficiency

SEM: standard error of the mean

SP4: single positive CD4

SP8: single positive CD8

TEC: thymic epithelial cell

TCR: T cell receptor

Vg/Dg : vector genomes/ diploid genomes

ZAP-70: Zeta-associated protein of 70kDa

INTRODUCTION

Primary immunodeficiency diseases (PID) consist of a heterogeneous group of more than 200 genetic disorders[1], with severe combined immunodeficiency (SCID) characterized by defective T and B lymphocyte function. Transplantation of histocompatible hematopoietic stem cells (HSCs) is the optimal treatment for infants with SCID but in the absence of histocompatible donors, these patients typically receive an HSC transplant from HLA-haploidentical donors. In the latter case, T cells are extensively depleted from the graft in an effort to prevent graft versus host disease (GvHD). Although recent modifications of this protocol have resulted in an increased survival rate, significant short-term and long-term complications are still reported and the lag time during which the patient remains susceptible to infections is quite long[2]. Thus, although this treatment is generally successful, it remains important to develop new therapeutic approaches.

Significant efforts have gone into developing gene therapy strategies for these patients. Indeed, gene therapy trials for X-SCID and more recently for adenosine deaminase-deficiency and Wiskott-Aldrich demonstrated that this strategy can cure human disease and they have continued to marketing approval[3-12]. The selective advantage of corrected progenitors and the massive expansion of corrected T cells has facilitated this success. Adverse events due to insertional mutagenesis of gammaretroviral vectors[13-16] have resulted in the development of lentiviral-based clinical trials for SCID patients. Notably, mutagenesis has not been reported in the latter [5, 17, 18] but it is still important to continue to explore and develop new therapeutic strategies.

Following transplantation of SCID patients with allogeneic healthy HSCs or gene-corrected autologous HSCs, T lymphocyte differentiation occurs in the

thymus[19]. These HSCs, administered by intravenous (IV) injection, must continuously home to the thymus because under physiological conditions, thymic settling progenitors are only able to give rise to a single round of thymocyte differentiation[20-23]. Notably though, the intrathymic injection of HSCs as well as pro-T cells improves T cell differentiation in the thymus[24-31] and increases the expansion of supporting thymic epithelial cells[32]. Additionally, the thymus can be targeted by the direct injection of antigens or vectors expressing genes of interest[33-37], with recombinant Adeno-Associated Virus (rAAV) vectors transducing thymocytes with a 10-fold higher efficiency than lentiviral vectors [34,37]. Indeed, rAAV vectors hold great promise for gene transfer therapies because they are capable of infecting non-dividing cells and particles of high titer and purity can be produced[38-42].

rAAV vectors were initially developed as single stranded viral DNA vectors. The transduction efficiency of these “conventional” rAAV vectors, based on the AAV2 serotype, is known to be tissue-dependent with significant gene transfer in various tissues[43-48] but only low level infection of murine hematopoietic cells[49-51]. However, several AAV serotypes have exhibited increased ability to transduce HSCs[40, 52-56] and long-term transgene persistence has been detected [54, 55, 57].

In an attempt to achieve efficient gene transfer in the thymus and correct T cell deficiency, we evaluated *in situ* intrathymic gene transfer using rAAV2 vectors cross-packaged into AAV 8, 9 and 10 serotypes. Intrathymic administration of all 3 serotypes led to transgene expression in all thymocyte subsets but AAV8 exhibited the highest gene transfer efficiency, resulting in the transduction of up to 5% of all thymocytes. Using mice that are immunodeficient due to mutations in the ZAP-70 protein tyrosine kinase [58] as a paradigm, we found that the intrathymic injection of an AAV2/8-ZAP-70 vector resulted in the

development of gene-corrected mature thymocytes within 10 days of gene transfer. Concurrently, AAV8-ZAP-70 gene transfer promoted the development of the thymic medulla, containing AIRE-expressing medullary thymic epithelial cells (mTECs) that mediate T-cell tolerance. Furthermore, AAV-transduced T cells were detected in the peripheral circulation by 2 weeks and these T cells exhibited long-term function for greater than 10 months, responding robustly to T cell receptor (TCR) stimulation. Thus, the thymus immune niche can be shaped by an intrathymic AAV-based strategy, accelerating the restoration of its architecture and facilitating a transient thymocyte differentiation with long term peripheral T cell function.

METHODS

AAV vector stocks, harboring the GFP or ZAP-70 genes, were administered by intrathymic injection into WT C57Bl/6 mice and ZAP-$70^{-/-}$ mice as indicated. All animal experiments were performed in accordance with the recommendations of the CNRS Animal Care Committee and were consistent with the guidelines set by the Panel on Euthanasia (AVMA) and the NIH Guide for the Care and Use of Laboratory Animals. T cell reconstitution was monitored by flow cytometry and frozen thymic sections were stained as previously described[59]. Vector genomes were monitored by real time PCR, for integration analyses, we adopted a sonication-based linker-mediated PCR method as previously described [60, 61]. Anti-OVA IgG responses were evaluated following ovalbumin immunization, serum anti-ZAP-70 antibodies as well as anti-dsDNA, anti-RNP and anti-SSA antibodies were evaluated by enzyme-linked immunosorbent assay (ELISA), neutralizing antibodies were monitored as previously described[62] and gene expression (Foxp3, IL-10) was evaluated by qRT-PCR. TCR repertoire was evaluated by deep sequencing and data analyzed using R Studio. Screening for IgM/IgG reactivity against autoantigens was performed using autoantibody arrays[63, 64].

RESULTS

Intrathymic AAV8 gene therapy reconstitutes the thymus architecture within 1.5 weeks and promotes a transient thymocyte differentiation

We first assessed the potential of self-complementary rAAV2 vectors (scAAV) harboring the GFP transgene and pseudotyped with the 8, 9 and 10 capsid serotypes to transduce the murine thymus. Our analyses revealed thymocyte transduction by all 3 serotypes; efficiencies in non-conditioned immunocompetent mice ranged from 2-5% by three days post injection (**Fig 1, A**). Transduced cells were found in all subsets, including the most immature $CD4^-CD8^-$ double negative (DN), double positive (DP) and the most mature single positive (SP) CD4 (SP4) and CD8 (SP8) thymocytes (**Fig 1, A, B**). Mice transduced with AAV9 vectors exhibited lower levels of DP thymocytes, within both the non-transduced and transduced subsets, suggesting a possible toxicity (**Fig 1, A, B**). However, total thymocyte numbers were not significantly altered, with a mean of $180x10^6$/ thymus. Furthermore, in mice undergoing IT administration with the AAV2/8 vector, the repartition of thymocyte subsets remained stable (**Fig 1, B**).

Following transduction of thymocytes, mature SP4 and SP8 thymocytes migrated to the periphery, strikingly representing up to 1% of peripheral T lymphocytes in lymphoid-replete WT mice at day 10 (**Fig 1, C**). However, gene-transduced peripheral T cells decreased by 2-fold at day 30, likely due to the emigration of newly differentiated mature thymocytes. Given the high-level transduction of thymocytes by AAV8, including immature DN thymocyte

progenitors, we studied the potential of this serotype to correct thymocyte differentiation in an immunodeficient mouse model.

Using a model of ZAP-70-deficient mice, exhibiting an arrest in thymocyte differentiation at the DP stage (reviewed in [58]), we assessed whether the IT administration of an AAV8 vector could be used to efficiently achieve gene transfer in defective thymocytes. Importantly, 3 days following IT transfer of the AAV2/8-GFP vector used above (**Fig 1, A**), the transduction of both DN and DP thymocytes was detected (**Fig 1, D**). Notably, gene transfer was detected in 2-5% of ZAP-$70^{-/-}$ thymocytes, resulting in the transduction of a mean of $0.8x10^6$ DN thymocytes and $4.6x10^6$ DP thymocytes (n=11, **Fig 1, D**). Thus, the level of IT AAV8 transduction in thymocytes of ZAP-$70^{-/-}$ immunodeficient mice was similar to that detected in WT mice, supporting the utilization of this strategy for gene transfer.

Defects in the development of SP thymocytes, irrespective of the mutation, result in a lack of a functional thymic medulla and it is likely that these stromal abnormalities contribute to immune dysregulation in the thymus (reviewed in[65, 66]). Defective medulla formation is classically associated with a lack of mTECs expressing the autoimmune regulator (AIRE). Its absence results in an aberrant T-cell selection[67] and the subsequent development of autoreactive T cells (reviewed in[68, 69]). Using a transgenic model, it has been shown that the leaky differentiation of as few as $3.5x10^5$ non-transgenic SP4 thymocytes, bearing TCRs with reactivities against self-antigens, is sufficient for the formation of a functional medulla[70]. As we detected the transduction of $>1x10^6$ DN/DP thymocytes in ZAP-$70^{-/-}$ mice using an AAV8 gene transfer approach **(Fig 1, E),** we hypothesized that an IT AAV8 gene therapy strategy might promote the generation of sufficient SP4 thymocytes for medulla formation. We therefore assessed whether thymic architecture is modified by the intrathymic

administration of single-stranded (ss) AAV8-ZAP-70 virions (1-3x10^{13} vector genomes (vg)/kg). In the absence of gene transfer, thymi of ZAP-$70^{-/-}$ mice harbored only a minimal medulla with a mean of 115 $AIRE^+$ cells/mm^2 of tissue (**Fig 2, A, B**). Notably, within 10 days following IT AAV8-ZAP-70 gene transfer, there was a dramatic generation of medullary tissue and the number of $AIRE^+$ mTECs significantly increased to 295/mm^2 of tissue ($p<0.001$; **Fig 2, A, B**). While the numbers of $AIRE^+$ cells decreased between 3 and 10 weeks post IT AAV8-ZAP-70 gene transfer (154/mm^2 to 95/mm^2), they remained significantly higher than those in age-matched ZAP-$70^{-/-}$ mice treated with control AAV8-GFP vector ($p<0.05$; **Fig 2, B**). Moreover, medulla development was robust, increasing from <0.03 mm^2 to 0.06 mm^2 by 1.5 weeks post gene transfer ($p<0.01$, **Fig E1, A**). It is interesting to note that medullary area remained significantly elevated for the first 3 weeks post gene transfer but then decreased at week 10, suggesting a transient thymic reconstitution (**Fig E1, A**).

As medulla formation and the generation of $AIRE^+$ mTECs are dependent on a cross-talk with mature SP thymocytes (reviewed in[65, 66,68, 69]), these data strongly suggested that T cell differentiation proceeded rapidly following IT gene delivery. Furthermore, mTEC turnover is estimated at 2-3 weeks[71, 72], suggesting that the decrease in $AIRE^+$ cells that we observed at 10 weeks post gene transfer (**Fig 2, B**) was associated with a single wave of thymocyte differentiation. Indeed, within the WT thymus, the percentages of gene-transduced cells that represented mature SP4 and SP8 thymocytes peaked at day 10 following gene transfer, likely representing the maturation of DP thymocytes[27, 73, 74], and decreased by 3 weeks, consistent with SP thymocyte emigration[75] (**Fig 1, C** and **2, C**, $p<0.01$). Differentiation of SP4 and SP8 thymocytes was detected in AAV8-ZAP-70-treated ZAP-$70^{-/-}$ mice but was not associated with a significant change in total thymocyte numbers, likely due to similar initial thymocyte numbers in the WT and KO mice (**Fig E1, B**). Notably,

the maturation of gene-transduced SP8 thymocytes in IT AAV8-ZAP-70-corrected ZAP-70$^{-/-}$ mice followed a similar kinetics to that detected in WT mice (**Fig 2, C**). SP4 thymocytes peaked even earlier, at 3 days post transduction (**Fig 2, C**, $p<0.01$, right panel). These data are in agreement with the kinetic signaling model of thymocyte differentiation wherein all DP thymocytes are first signaled to an intermediate SP4 thymocyte fate, before SP8 differentiation [76]. Mature SP thymocytes were detected at all time points in WT mice, but as expected from the physiological involution of the thymus with age, the absolute numbers of SP thymocytes decreased between 0.5 (3 days) and 3 weeks post gene transfer (note that mice were 3 weeks of age at the time of gene transfer; **Fig 2, D**). The total numbers of SP thymocytes in ZAP-70$^{-/-}$ mice following AAV8-ZAP-70 gene transfer were greater than $2x10^6$ at 3 days post gene transfer (**Fig 2, D**). Consistent with the gradual loss of AIRE$^+$ cells and the decreasing medulla size following IT gene correction (**Fig 2, B**), SP thymocytes decreased to baseline levels at 3 weeks (**Fig 2, D**). Together these data strongly suggest that intrathymic AAV gene correction provides for a single wave of thymocyte differentiation.

Intrathymic AAV8-ZAP-70 transduction promotes long term maintenance of peripheral T cells and T lineage-specific gene transfer

Consistent with the kinetics of thymocyte differentiation and emigration[27, 73, 75, 77], gene-corrected T cells were detected in the blood stream within 3 weeks following IT transfer (**Fig 3, A**). T cells were monitored in peripheral blood samples between 3 and 40 weeks post transduction. It is notable that a single wave of T cell differentiation allowed for the maintenance of a stable level of peripheral T cells for the 40 week evaluation period (>10 months). AAV8-ZAP70-transduced KO mice exhibited a significantly higher percentage of peripheral T cells relative to KO or IT:AAV8-ZAP-70 transduced KO mice at all

time points evaluated; 3-10 weeks, 11-20 weeks, 21-30 weeks and 31-40 weeks ($p<0.0001$ for all time points, **Fig 3, A**).

The thymus is the site of T cell differentiation but B cells and hematopoietic progenitors with myeloid lineage potential are also present in this organ[78, 79]. Furthermore, AAV virions can diffuse, potentially resulting in the transduction of other cell types (reviewed in[80, 81]). It was therefore important to compare the transduction of T cells and non-T cells by AAV8-ZAP-70 virions following intrathymic gene transfer. As expected, almost 100% of all peripheral T cells, encompassing both CD4 and CD8 subsets, expressed the AAV8-encoded ZAP-70 transgene (**Fig 3, B**). Notably though, transgene expression was not detected in significant levels in non-T cell hematopoietic lineages, including B cells and myeloid cells, nor in the bone marrow during the entire 40 week follow up period (**Fig 3, B**). Furthermore, expression levels of ectopic ZAP-70 in gene-transduced peripheral T cells were approximately 2-4-fold higher than endogenous levels, monitored as a function of MFI, and these levels did not significantly change during the 40 week follow up (**Fig 3, C**).

We next assessed whether the maintenance of transduced T cells in the peripheral circulation was associated with a stable percentage and number of $CD3^+$ T cells in the lymph nodes of AAV8-ZAP-70-treated mice (**Fig 3, D**). While T cell levels were significantly lower than those detected in WT mice, both in percentages and absolute numbers, they were induced by 3 weeks post intrathymic transduction, revealing the rapid initial wave of AAV-transgene-mediated thymocyte differentiation. Furthermore, they remained stable for >10 months. The progression of immature DP thymocytes through positive selection requires ZAP-70-dependent TCR signaling[82,83]. Positively selected DP thymocytes then undergo CD4/CD8 lineage choice, a complex process that has been shown to occur through kinetic signaling: Under conditions of persistent

TCR signaling, CD4 T cell differentiation occurs whereas MHC-class I-specific CD8 T cells only differentiate following a disruption of MHC-class II/TCR signals and subsequent cytokine signaling[84, 85]. Interestingly, in the presence of high levels of ectopic ZAP-70 from the AAV8-ZAP-70 vector (**Fig 3, C**), both the thymic and peripheral CD4/CD8 ratios in AAV8-ZAP-70-treated mice was significantly skewed to a CD4 lineage fate ($p<0.05$; **Fig 2, D and 3, E**).

Intrathymic AAV gene transfer results in the development of T cells with integrated AAV8-ZAP-70 vectors and diverse αβ T cell receptor clonotypes

The persistence of gene-transduced T cells for >40 weeks was surprising in light of high level T cell proliferation and the propensity of AAV vectors to remain episomal [86]. We therefore first assessed vector copy numbers in peripheral T cells and determined that they ranged from approximately 0.1 to 1 vector genomes per diploid genome (Vg/Dg), at time points ranging between 3 to 43 weeks post intrathymic gene transfer (**Fig 4, A**). The low copy number suggested that the vector was integrated but to further assess this point, AAV8-ZAP-70-reconstituted T cells were TCR-stimulated and copy number was evaluated. TCR-stimulated AAV8-ZAP-70-reconstituted T cells proliferated robustly, as monitored by dilution of the CTV proliferation dye, demonstrating a reconstituted TCR signaling cascade (**Fig 4, B**). Moreover, while the vast majority of reconstituted T cells underwent >4 divisions, AAV copy number (Vg/Dg) was not significantly altered, strongly pointing to vector integration (**Fig 4, B**).

To directly assess vector integration, genomic DNA was fragmented by sonication (to avoid biases caused by the non-random distribution of restriction sites on the genome), ligated to a barcoded linker cassette prior to PCR amplification, and evaluated via sonication linker-mediated (SLiM) PCR.

Nested PCR with vector and linker cassette specific oligonucleotides allowed detection of PCR products with at least two different primers in LN samples from 3 of 6 IT:AAV8-ZAP-70-transduced mice (and 2 of 2 mice at 43 weeks post gene transfer; **Fig 4, C**). Thus, integrated AAV is likely to be responsible for driving ZAP-70 expression in peripheral T cells, under conditions of long-term persistence and TCR stimulation.

The potential of differentiated T cells to recognize a large array of foreign proteins is fostered by the unparalleled diversity of the TCR with recombined α and β polypeptide chains allowing for the generation of $>10^{15}$ unique receptors[87]. However, under conditions of limited thymocyte differentiation, repertoire diversity can be reduced[34]. Furthermore, infections and tumors can drive an antigen-mediated bias in αβ TCR repertoires (reviewed in[88]). While only few studies have monitored TCR repertoires in patients or mice treated with rAAV vectors, the robust T cell response against an AAV transgene in one trial was shown to be associated with a biased TCRBV repertoire[89]. It was therefore of important to assess the repertoire diversity in our gene corrected mice. As expected, the numbers of detected TRA sequences in KO as well as AAV8-GFP-transduced mice was minimal. However, they increased rapidly following ZAP-70 gene transfer (Day 10, **Fig 4, D**). TCR repertoire diversity was lower than that of WT mice but the number of distinct TRAV, TRAJ, TRBV, and TRBJ clonotypes increased until 3 weeks post gene transfer and remained stable until 43 weeks (**Fig 4, D**). In WT mice, clonotype distribution was not yet fully diverse at day 10 of life, being made up of a few mildly expanded TCRs. By week 3, WT mice exhibited repertoires that were fully diverse, with 1-3 copies per clonotype (**Fig 4, D, bottom**). The repertoires of AAV8-ZAP-70-reconstituted mice were less diverse than WT mice, with an expansion of some clonotypes, but a diverse population of TCRs was detected (**Fig 4, D**).

Induction of humoral immunity in IT-AAV8-ZAP-70-treated mice

To determine whether AAV8-ZAP-70-tranduced mice can mount an immune response, mice were immunized with ovalbumin (OVA) at a late time point post gene transfer (46 weeks). At this time point, neither WT nor KO mice harbored OVA-specific antibodies. Notably though, mice that were intrathymically transduced with AAV8-ZAP-70 but not AAV8-GFP generated a significantly higher level of anti-OVA IgG antibodies by 6 weeks post immunization (1:2,000 dilution, $p<0.001$, **Fig 5, A**). While antibody generation was lower than that detected in WT mice, AAV8-ZAP-70-transduced mice were already 1 year post gene transfer and the level of IgG generation was highly significant relative to KO mice ($p<0.001$; **Fig 5, A**).

Changes in TCR repertoire distribution can result from immune responses against AAV capsid epitopes as well as the expressed transgene (reviewed in[90]). Furthermore, different rAAV serotypes have induced T-cell-dependent and –independent anti-capsid humoral responses[91], even when injected into an immune-privileged organ such as the brain[92]. We therefore monitored the presence of anti-capsid antibodies in IT AAV8-treated ZAP-$70^{-/-}$ mice as a function of neutralization; neutralizing factors were defined as serum dilutions that inhibited AAV8 infection by >50%. No control ZAP-$70^{-/-}$ mice harbored neutralizing antibodies and at a 1/100 dilution, antibodies were not detected in IT AAV8-ZAP-70-treated ZAP-$70^{-/-}$ mice. However, at a 1/10 dilution, 10 of 14 IT AAV8-ZAP-70-treated ZAP-$70^{-/-}$ mice were positive between 3 and 17 weeks post transduction (71%). Notably though, at this dilution, anti-AAV8 neutralizing activity was also detected in a high percentage of IT AAV8-GFP-treated ZAP-$70^{-/-}$ mice; mice that do not have peripheral T cells (4 of 5, 80%; **Fig 5, B**). Thus, the intrathymic injection of the AAV8 serotype induces a low level T cell-independent anti-capsid humoral response.

We next assessed whether the reconstituted mice exhibited an immune response against the ZAP-70 transgene. The intrathymic expression of the injected transgene likely minimizes an immune response, enhancing the deletion of autoreactive thymocytes[33, 35], but our findings of a T cell-independent anti-capsid neutralizing activity (**Fig 5, B**) suggested the possibility of an anti-transgene response. While anti-ZAP-70 antibodies were not detected at 3 weeks post AAV8-ZAP-70 transduction, 5 of 7 mice harbored antibodies at 10 weeks (>25 ng/ml sera; $p<0.01$). Mean antibody levels then decreased at 17 weeks (from 58 to 34 ng/ml) and by 43 weeks, antibody levels were <30ng/ml (n=5, **Fig 5, C**) and ZAP-70 protein did not elicit T cell activation (data not shown). In conclusion, anti-transgene antibodies were produced at early time points following intrathymic transduction but levels decreased and were sufficiently low that they did not result in the elimination of gene-transduced T lymphocytes (**Fig 2, B**).

Patients with primary immunodeficiencies often present autoimmune manifestations and both immunodeficient patients and mice have been shown to produce a diverse range of autoantibodies[64, 93]. We therefore assessed whether gene-corrected ZAP-70-/- mice produced autoantibodies. Using an autoantigen microarray containing 123 different autoantigens, we did not observe increased levels of autoantibody production in age-matched ZAP-70$^{-/-}$ mice as compared to control mice. However, IT injections of both control AAV8-GFP and AAV8-ZAP-70 vectors resulted in the induction of IgM antibodies against a broad panel of autoantigens by 3 weeks post gene transfer (**Fig E2)**. IgG antibodies were significantly higher in IT AAV8-ZAP-70-transduced mice, in accord with the requirement of functional T cells for immunoglobulin class switching. IgG autoantibodies peaked at 10 weeks post transduction[63, 64] (**Fig 6, A**). Importantly though, absolute levels of antibodies against 3 tested autoantigens (double-stranded DNA (dsDNA), ribonucleoprotein (RNP), and

Sjögren's-syndrome-related antigen A (SSA)) were significantly lower in AAV8-ZAP-70-transduced mice at both 10 weeks and 43 weeks post gene transfer than in MRL/*lpr* mice which spontaneously develop a systemic lupus erythematosus (SLE)-like syndrome. Furthermore, levels in AAV8-ZAP-70-transduced mice were not significantly higher than that detected in control MRL/MpJ mice (**Fig 6, B**). Thus, intrathymic AAV8 administration induces a rapid but low-level, broad spectrum of autoantibodies that decreases with time. Notably, these low levels of autoantibodies did not result in pathological consequences as mice survived for over 50 weeks without overt autoimmune manifestations.

Intrathymic AAV8-ZAP-70 gene transfer results in the differentiation of effector and regulatory T cell subsets

Under conditions of lymphopenia, naive T cells proliferate in response to weak TCR interactions with self-peptide/MHC complexes, differentiating into memory-like T cells in the absence of antigenic stimulation (reviewed in[94]). It was therefore important to study the phenotype of peripheral T cells in IT-AAV8-ZAP-70-reconstituted mice. Notably, reconstituted mice exhibited a significant increase in $CD62L^{-}CD44^{+}$ effector memory T cells as compared to the majority of $CD62L^{+}CD44^{-}$ naïve T cells in WT mice. This biased ratio of memory: naive T cells was detected throughout the experimental period of 10 months (**Fig 7, A**). Thus, in our study, a single wave of thymocyte differentiation following IT-AAV8-ZAP-70 gene transfer resulted in the peripheral differentiation of polyclonal T lymphocytes with a memory/effector phenotype.

To determine the potential effector function of AAV8-ZAP-70-transduced T cells, we first assessed *in vivo* cytokine levels. *In vivo*, there was a transient increase in TNF-α and IFN-γ levels at 3 weeks post AAV8 transduction (**Fig E3, A**), correlating with the induction of a low-level humoral response (**Fig 6, A and**

E2). However, cytokine levels then returned to baseline by 10 weeks (**Fig E3, A**), consistent with the decrease in autoantibodies. We next examined the ability of peripheral AAV8-ZAP70-reconstituted T cells to secrete cytokines upon anti-CD3/anti-CD28 mAb activation. IL-17, TNF-α and IFN-γ were secreted by T cells from AAV8-ZAP70-reconstituted mice by 3 weeks after gene transfer and secretion of all 3 cytokines was significantly higher than that detected in KO mice by 10 weeks (n=3-10 mice per time point, **Fig 7, B**; $p<0.05$, $p<0.001$). As compared to WT peripheral T cells, IL-17 was the only cytokine that was significantly higher in gene-corrected mice (**Fig 7, B**; $p<0.05$). Thus, peripheral AAV8-ZAP70-reconstituted T cells were competent to secrete cytokines following *ex vivo* TCR stimulation.

Despite high *ex vivo* TCR-induced cytokine secretion, *in vivo* cytokine levels were not elevated and AAV-reconstituted mice did not exhibit autoimmune symptoms. It was therefore important to assess whether gene-corrected regulatory T cells (Treg) controlled immune responsiveness in these mice. Notably, the development of Tregs expressing the Foxp3 transcription factor is dependent on a thymic medulla[95], a structure which was restored by day 10 of gene transfer (**Fig 2, A**). Accordingly, by 3 weeks post gene transfer, Tregs were detected in the peripheral circulation of AAV8-ZAP-70-treated mice at levels similar to those in WT mice (**Fig 7, C**). Notably, by 10 weeks post IT gene transfer, the percentages of Tregs were significantly higher in AAV8-ZAP-70-treated mice than in WT mice (**Fig 7, C**; $p<0.05$). Importantly, these T cells exhibited an activated phenotype as monitored by significantly higher levels of Treg markers including CTLA4, GITR and CD39 (n=5 per group, **Fig E3, B**). As regards function, sorted $CD4^+CD25^{Hi}$ cells from both WT and AAV8-ZAP-70-transduced cells revealed equivalent levels of Foxp3 transcripts (n=12) but IL-10 levels were significantly higher in the latter ($p<0.05$; **Fig 7, D**). Furthermore, IL-10 levels were significantly higher in conventional ($CD4^+CD25^-$ T cells) from

reconstituted mice than WT mice (n=6-9; $p<0.005$). Thus, a high suppressive environment in reconstituted regulatory T cells likely restrains *in vivo* immune activation following AAV8-ZAP-70 gene transfer.

DISCUSSION

Thymocyte development is dependent on the thymic stroma, composed of thymic epithelial cells (TECs) and non-epithelial cells that together form an organized 3-dimensional network[96]. The intercellular communications between developing thymocytes and TECs result in a thymus architecture that allows the generation of a diverse and self-tolerant pool of mature T cells. In SCID patients as well as in cancer patients with thymus damage, an abnormal thymic architecture negatively impacts on thymocyte differentiation (reviewed in[19, 65, 66, 97]). Here, we show that an intrathymic AAV8 gene correction results in a remarkable generation of mTECs and the development of a medullary architecture in ZAP-70-deficient mice, within 10 days of vector administration. Moreover, the absolute number of mTECs expressing AIRE increased by 3-fold in this period. AIRE is critical for immune tolerance, promoting the deletion of self-reactive thymocytes and the development of regulatory T cells[65, 66, 68, 69]. Therefore, to date, the IT AAV gene transfer strategy described here appears to be the most rapid regulator of thymic architecture in immunodeficient mice.

As the crosstalk between mTECs and developing thymocytes is required for T cell maturation, extensive research has focused on the identification of factors, conditions and cell types that enhance mTEC reconstitution (reviewed in[98]). The differentiation of autoreactive mature CD4 thymocytes regulates the formation and organization of the medulla in an antigen-dependent manner as shown by the importance of the CD28–CD80/86 and CD40–CD40L costimulatory pathways as well as RANK-RANKL and LTαβ-LTβR interactions (reviewed in [68]). Furthermore, sex steroid ablation was found to enhance thymocyte differentiation by increasing Notch ligand expression on TECs[99-101] while keratinocyte growth factor (KGF), IL-22, Bmp4 and FoxN1 directly promote TEC proliferation and survival[102-104]. Specific cell types such as pro-T

cells facilitate thymus reconstruction[32, 105, 106] while innate lymphoid cells induce an IL-22–mediated TEC survival[107]. Chemokines can also facilitate thymic reconstitution; under conditions of thymic damage, CCL21 treatment of hematopoietic progenitors rescues their migration while a combined inhibition of p53 and KGF increases intrathymic CCL21 expression and TEC recovery[108, 109]. Notably though, the success of these approaches often requires a significant lag time whereas an IT AAV gene strategy corrected the medullary microenvironment within <10 days, concomitant with a correction of the T cell deficiency and the differentiation of SP4 thymocytes. It will be of interest to determine whether a combined approach, concomitantly correcting a T cell deficiency and the medullary microenvironment[59], further promotes reconstitution. Furthermore, AAV can be used to deliver TEC-inducing molecules to patients suffering from suboptimal T cell differentiation—for example, boosting thymocyte differentiation in HSC-transplanted cancer patients by IT AAV administration of the IL-22 cytokine. This type of intrathymic targeting approach, by ultrasound-mediated guidance, has been shown to be minimally invasive and safe in both mice and macaques[28, 31, 37, 110]. Further studies, focused on the intrathymic administration of vectors and hematopoietic progenitor cells into non-human primates by interventional radiologists, will help to establish the clinical framework in which this type of therapeutic strategy can be developed.

AAV vectors have successfully been used to achieve gene transfer in numerous tissues[81]. Nevertheless, studies of AAV gene transfer in the hematopoietic system have been more sparse, likely due to the extensive division of these cells. However, AAV1, modified AAV6 and AAV7 vectors have been found to efficiently transduce HSCs[54, 57, 111, 112]. Furthermore, we show here that AAV8, 9 and 10 serotypes promote efficient thymocyte transduction. While the property of AAV vector genomes to exist primarily as episomes would

be expected to negatively affect their ability to be used for a stable gene therapy in dividing cells, long-term persistence of transgene expression has been detected in HSCs[54, 55, 57]. Moreover, it has recently been shown that T lymphocytes represent the *in vivo* site of AAV persistence following natural infection[113]. This is likely linked to the AAV vector-mediated long-term transgene maintenance (>10 months) that we detected in gene-corrected T lymphocytes. Indeed, our findings that AAV vector copy number in reconstituted T cells was approximately 1 and that long-term reconstituted T cells harbored integrated vector is likely to broaden the scope of immunological deficiencies for which this type of approach can be envisioned. As persistence of intrathymic-injected progenitors with a specific T cell receptor gene provided for life-long immunity[31], it will be of interest to determine whether the direct targeting of thymocytes with an AAV8-encoded tumor-specific TCR or chimeric antigen receptor (CAR) will promote an anti-tumor response that is superior to that currently achieved by ex vivo manipulation of peripheral T cells.

Immune responses against AAV capsid serotypes as well as expressed transgenes have hampered the success of AAV gene therapy trials (reviewed in[114]). Even following AAV injections into regions that are considered to be immune-privileged such as the brain[92] or the intravitreal space[115, 116], anti-capsid antibodies have been detected. Nevertheless, the development of immunosuppressive treatments has protected against AAV capsid immunity [117, 118,119]. Indeed, long-term transgene expression has been observed following the systemic AAV administration of genes such as myotubularin[120, 121] and microdystrophin[122], promoting AAV-based treatments for patients with X-linked myotubular myopathy and Duchenne muscular dystrophy, respectively.

While T cell immunity can provoke anti-AAV reactivity, it can also limit pathological responses. The recruitment of suppressive regulatory T cells as

well as organ-specific T cell exhaustion can result in extended transgene expression[123,124]. While we initially hypothesized that the direct administration of AAV into the thymus would result in the deletion of autoreactive thymocytes and the subsequent absence of an immune response[33, 35], we detected low level humoral responses to both the AAV8 capsid and the ZAP-70 transgene. Interestingly, anti-capsid responses were induced at similar levels in ZAP-70$^{-/-}$ mice treated by IT administration of the control AAV8-GFP vector. As T cell differentiation did not proceed in these latter mice, these data indicate the development of a T cell-independent immune response. In contrast, IgG autoantibodies were generated in AAV gene-corrected ZAP-70$^{-/-}$ mice, pointing to the importance of T cells in immunoglobulin class switching. Moreover, similarly to patients where AAV transduction correlated with increases in specific TCRBV families[123], the humoral immune response in IT AAV8-ZAP-70-treated mice was associated with a diverse but biased TCR repertoire. Notably though, the levels of generated autoantibodies were significantly lower than that detected in SLE-prone MRL/*lpr* mice and none of the IT gene therapy-treated mice developed symptoms of autoimmune disease during the 10 month follow up period. This is likely due to 1) the low and transient nature of the autoantibody response and 2) the extensive differentiation of AAV-corrected thymocytes to a Treg fate. Notably, AAV gene transfer resulted in a T effector/Treg ratio that allowed for a balanced immune homeostasis.

Combination therapies will likely optimize life-long T cell differentiation in SCID patients and T cell reconstitution in cancer patients. An ideal treatment will promote 1) HSC expansion, 2) the migration and entry of hematopoietic progenitors into the thymus 3) a thymus architecture that is conducive to thymocyte maturation and 4) the selection of a broad-based repertoire of self-tolerant effector and regulatory T cells. One bottleneck is progenitor entry as the thymus is not continually receptive to the import of hematopoietic

progenitors, at least in mice[125, 126]. Furthermore, irradiation reduces progenitor homing by >10-fold[109]. While this bottleneck can be partially overcome by injecting HSCs or hematopoietic progenitors directly into the thymus[24, 27, 28, 31, 110, 127, 128], histocompatible donors are not always available. Our study reveals the potential of an IT AAV8 gene therapy strategy to promote an extremely rapid reconstitution of the thymus microenvironment and the differentiation of mTEC-dependent regulatory T cells within a 7-10 day period.

In our studies, a single wave of thymocyte differentiation promoted the long-term maintenance of peripheral gene-corrected T cells. Indeed, in several "experiments" of nature", patients with mutations that generally result in a SCID phenotype were found to be relatively healthy with significant T cell numbers, due to a reversion mutation. As this type of event is statistically improbable, it is likely that the peripheral T cell reconstitution detected in these patients (with mutations in WAS, RAG1, LAD, NEMO, CD3zeta, γc and ADA) is due to a reversion mutation in a single hematopoietic progenitor[129-141]. While these data strongly support the hypothesis that gene correction of a very limited number of thymic progenitors can give rise to a large number of peripheral T cells, it remains to be determined whether T cells in these patients are due to a single wave of thymocyte differentiation. Moreover, in the context of an intrathymic gene transfer approach, it will be important to assess whether the remnant thymus present in many patients with SCID as well as the natural process of thymic involution would negatively impact on the type of therapeutic strategy described here. Importantly, we found that intrathymic gene transfer into Rag2-/- mice with a remnant thymus is feasible by a surgical approach but the success of intrathymic HSC transfer into older mice with an involuted thymus is significantly reduced (our unpublished observations). Thus, a combination therapy of intrathymic AAV gene transfer, promoting a restoration of the thymic architecture and medulla formation, followed by an intravenous HSC

transplantation, allowing long term T cell differentiation in a reconstituted thymus, may presents a novel approach for the treatment of immunodeficient patients requiring a rapid T cell reconstitution.

Acknowledgements

We thank all members of our lab for their scientific critique and support. The authors thank the Center for Production of Vector (CPV- vector core from University Hospital of Nantes / French Institute of Health (INSERM) / University of Nantes) http://umr1089.univ-nantes.fr/plateaux-technologiques/cpv/centre-de-production-de-vecteurs-2194757.kjsp?RH=1518531897125 and are grateful to Myriam Boyer of Montpellier Rio Imaging for support in cytometry experiments, Léo Garcia for his assistance in bioinformatic analyses, Luz Blanco and Mariana Kaplan for generously providing serum from autoimmune MRL/*lpr* mice and providing advice on ELISAs and the ZEFI staff for their support of animal experiments.

Author Contributions

M.P., O.A., N.T. and V.S.Z. conceived the study. M.P., A.M., M.G., S.G. and V.S.Z. designed, performed and analyzed the experiments. M.I. and A.S. performed and analyzed histological analyses; TCR repertoire analysis was performed by P.B. and D.K.; D.C., F.B., A.S. and E.M. designed and performed the integration analyses; and I.R. and P-Z.L. performed the autoantibody microaaray analyses. M.P, N.T. and V.S.Z. wrote the manuscript and A.M., M.I. and O.A. provided important critical review.

REFERENCES

1. Al-Herz W, Bousfiha A, Casanova JL, Chatila T, Conley ME, Cunningham-Rundles C, et al. Primary immunodeficiency diseases: an update on the classification from the international union of immunological societies expert committee for primary immunodeficiency. Front Immunol. 2014;5:162.
2. Heimall J, Puck J, Buckley R, Fleisher TA, Gennery AR, Neven B, et al. Current Knowledge and Priorities for Future Research in Late Effects after Hematopoietic Stem Cell Transplantation (HCT) for Severe Combined Immunodeficiency Patients: A Consensus Statement from the Second Pediatric Blood and Marrow Transplant Consortium International Conference on Late Effects after Pediatric HCT. Biol Blood Marrow Transplant. 2017; 23(3):379-387.
3. Fischer A, Hacein-Bey-Abina S, Cavazzana-Calvo M. Gene therapy for primary immunodeficiencies. Hematology/oncology clinics of North America. 2011;25(1):89-100.
4. Aiuti A, Cattaneo F, Galimberti S, Benninghoff U, Cassani B, Callegaro L, et al. Gene therapy for immunodeficiency due to adenosine deaminase deficiency. N Engl J Med. 2009;360(5):447-58.
5. Aiuti A, Biasco L, Scaramuzza S, Ferrua F, Cicalese MP, Baricordi C, et al. Lentiviral hematopoietic stem cell gene therapy in patients with Wiskott-Aldrich syndrome. Science. 2013;341(6148):1233151.
6. Mukherjee S, Thrasher AJ. Gene therapy for PIDs: progress, pitfalls and prospects. Gene. 2013;525(2):174-81.
7. Fischer A, Hacein-Bey-Abina S, Cavazzana-Calvo M. Gene therapy of primary T cell immunodeficiencies. Gene. 2013;525(2):170-3.
8. Hacein-Bey Abina S, Gaspar HB, Blondeau J, Caccavelli L, Charrier S, Buckland K, et al. Outcomes following gene therapy in patients with severe Wiskott-Aldrich syndrome. JAMA. 2015;313(15):1550-63.
9. Pala F, Morbach H, Castiello MC, Schickel JN, Scaramuzza S, Chamberlain N, et al. Lentiviral-mediated gene therapy restores B cell tolerance in Wiskott-Aldrich syndrome patients. J Clin Invest. 2015;125(10):3941-51.
10. Castiello MC, Scaramuzza S, Pala F, Ferrua F, Uva P, Brigida I, et al. B-cell reconstitution after lentiviral vector-mediated gene therapy in patients with Wiskott-Aldrich syndrome. J Allergy Clin Immunol. 2015;136(3):692-702 e2.
11. Shaw KL, Garabedian E, Mishra S, Barman P, Davila A, Carbonaro D, et al. Clinical efficacy of gene-modified stem cells in adenosine deaminase-deficient immunodeficiency. J Clin Invest. 2017;127(5):1689-99.
12. Aiuti A, Roncarolo MG, Naldini L. Gene therapy for ADA-SCID, the first marketing approval of an ex vivo gene therapy in Europe: paving the road for the next generation of advanced therapy medicinal products. EMBO Mol Med. 2017;9(6):737-40.
13. Thrasher AJ, Gaspar HB, Baum C, Modlich U, Schambach A, Candotti F, et al. Gene therapy: X-SCID transgene leukaemogenicity. Nature. 2006;443(7109):E5-6; discussion E-7.
14. Hacein-Bey-Abina S, Garrigue A, Wang GP, Soulier J, Lim A, Morillon E, et al. Insertional oncogenesis in 4 patients after retrovirus-mediated gene therapy of SCID-X1. J Clin Invest. 2008;118:3132-42.
15. Howe SJ, Mansour MR, Schwarzwaelder K, Bartholomae C, Hubank M, Kempski H, et al. Insertional mutagenesis combined with acquired somatic mutations causes leukemogenesis following gene therapy of SCID-X1 patients. J Clin Invest. 2008;118(9):3143-50.
16. Stein S, Ott MG, Schultze-Strasser S, Jauch A, Burwinkel B, Kinner A, et al. Genomic instability and myelodysplasia with monosomy 7 consequent to EVI1 activation after gene therapy for chronic granulomatous disease. Nat Med. 2010;16(2):198-204.
17. De Ravin SS, Wu X, Moir S, Anaya-O'Brien S, Kwatemaa N, Littel P, et al. Lentiviral hematopoietic stem cell gene therapy for X-linked severe combined immunodeficiency. Sci Transl Med. 2016;8(335):335ra57.
18. Mamcarz E, Zhou S, Lockey T, Abdelsamed H, Cross SJ, Kang G, et al. Lentiviral Gene Therapy Combined with Low-Dose Busulfan in Infants with SCID-X1. N Engl J Med. 2019;380(16):1525-34.
19. Shah DK, Zuniga-Pflucker JC. An overview of the intrathymic intricacies of T cell development. J Immunol. 2014;192(9):4017-23.

20. Goldschneider I, Komschlies KL, Greiner DL. Studies of thymocytopoiesis in rats and mice. I. Kinetics of appearance of thymocytes using a direct intrathymic adoptive transfer assay for thymocyte precursors. J Exp Med. 1986;163(1):1-17.
21. Scollay R, Smith J, Stauffer V. Dynamics of early T cells: prothymocyte migration and proliferation in the adult mouse thymus. Immunol Rev. 1986;91:129-57.
22. Frey JR, Ernst B, Surh CD, Sprent J. Thymus-grafted SCID mice show transient thymopoiesis and limited depletion of V beta 11+ T cells. J Exp Med. 1992;175(4):1067-71.
23. Berzins SP, Boyd RL, Miller JF. The role of the thymus and recent thymic migrants in the maintenance of the adult peripheral lymphocyte pool. J Exp Med. 1998;187(11):1839-48.
24. Vicente R, Adjali O, Jacquet C, Zimmermann VS, Taylor N. Intrathymic transplantation of bone marrow-derived progenitors provides long-term thymopoiesis. Blood. 2010;115(10):1913-20.
25. Martins VC, Ruggiero E, Schlenner SM, Madan V, Schmidt M, Fink PJ, et al. Thymus-autonomous T cell development in the absence of progenitor import. J Exp Med. 2012;209(8):1409-17.
26. Peaudecerf L, Lemos S, Galgano A, Krenn G, Vasseur F, Di Santo JP, et al. Thymocytes may persist and differentiate without any input from bone marrow progenitors. J Exp Med. 2012;209(8):1401-8.
27. de Barros SC, Zimmermann VS, Taylor N. Hematopoietic stem cell transplantation: Targeting the thymus. Stem Cells. 2013.
28. Tuckett AZ, Thornton RH, O'Reilly RJ, van den Brink MRM, Zakrzewski JL. Intrathymic injection of hematopoietic progenitor cells establishes functional T cell development in a mouse model of severe combined immunodeficiency. J Hematol Oncol. 2017;10(1):109.
29. Zhang SL, Wang X, Manna S, Zlotoff DA, Bryson JL, Blazar BR, et al. Chemokine treatment rescues profound T-lineage progenitor homing defect after bone marrow transplant conditioning in mice. Blood. 2014;124(2):296-304.
30. Thordardottir S, Hangalapura BN, Hutten T, Cossu M, Spanholtz J, Schaap N, et al. The aryl hydrocarbon receptor antagonist StemRegenin 1 promotes human plasmacytoid and myeloid dendritic cell development from CD34+ hematopoietic progenitor cells. Stem Cells Dev. 2014;23(9):955-67.
31. Tuckett AZ, Thornton RH, Shono Y, Smith OM, Levy ER, Kreines FM, et al. Image-guided intrathymic injection of multipotent stem cells supports lifelong T-cell immunity and facilitates targeted immunotherapy. Blood. 2014;123(18):2797-805.
32. Smith MJ, Reichenbach DK, Parker SL, Riddle MJ, Mitchell J, Osum KC, et al. T cell progenitor therapy-facilitated thymopoiesis depends upon thymic input and continued thymic microenvironment interaction. JCI Insight. 2017;2(10).
33. DeMatteo RP, Chu G, Ahn M, Chang E, Barker CF, Markmann JF. Long-lasting adenovirus transgene expression in mice through neonatal intrathymic tolerance induction without the use of immunosuppression. J Virol. 1997;71(7):5330-5.
34. Adjali O, Marodon G, Steinberg M, Mongellaz C, Thomas-Vaslin V, Jacquet C, et al. In vivo correction of ZAP-70 immunodeficiency by intrathymic gene transfer. J Clin Invest. 2005;115(8):2287-95.
35. Marodon G, Fisson S, Levacher B, Fabre M, Salomon BL, Klatzmann D. Induction of antigen-specific tolerance by intrathymic injection of lentiviral vectors. Blood. 2006;108(9):2972-8.
36. Irla M, Saade M, Kissenpfennig A, Poulin LF, Leserman L, Marche PN, et al. ZAP-70 restoration in mice by in vivo thymic electroporation. PLoS One. 2008;3(4):e2059.
37. Moreau A, Vicente R, Dubreil L, Adjali O, Podevin G, Jacquet C, et al. Efficient intrathymic gene transfer following in situ administration of a rAAV serotype 8 vector in mice and nonhuman primates. Mol Ther. 2009;17(3):472-9.
38. Le Bec C, Douar AM. Gene therapy progress and prospects--vectorology: design and production of expression cassettes in AAV vectors. Gene Ther. 2006;13(10):805-13.
39. Russell DW. AAV vectors, insertional mutagenesis, and cancer. Mol Ther. 2007;15(10):1740-3.
40. Buning H, Huber A, Zhang L, Meumann N, Hacker U. Engineering the AAV capsid to optimize vector-host-interactions. Curr Opin Pharmacol. 2015;24:94-104.
41. Brown N, Song L, Kollu NR, Hirsch ML. Adeno-Associated Virus Vectors and Stem Cells: Friends or Foes? Hum Gene Ther. 2017;28(6):450-63.
42. Chandler RJ, Sands MS, Venditti CP. Recombinant Adeno-Associated Viral Integration and Genotoxicity: Insights from Animal Models. Hum Gene Ther. 2017;28(4):314-22.

43. Kaplitt MG, Leone P, Samulski RJ, Xiao X, Pfaff DW, O'Malley KL, et al. Long-term gene expression and phenotypic correction using adeno-associated virus vectors in the mammalian brain. Nat Genet. 1994;8(2):148-54.
44. Kaplitt MG, Xiao X, Samulski RJ, Li J, Ojamaa K, Klein IL, et al. Long-term gene transfer in porcine myocardium after coronary infusion of an adeno-associated virus vector. Ann Thorac Surg. 1996;62(6):1669-76.
45. McCown TJ, Xiao X, Li J, Breese GR, Samulski RJ. Differential and persistent expression patterns of CNS gene transfer by an adeno-associated virus (AAV) vector. Brain Res. 1996;713(1-2):99-107.
46. Griffey MA, Wozniak D, Wong M, Bible E, Johnson K, Rothman SM, et al. CNS-directed AAV2-mediated gene therapy ameliorates functional deficits in a murine model of infantile neuronal ceroid lipofuscinosis. Mol Ther. 2006;13(3):538-47.
47. Sondhi D, Peterson DA, Giannaris EL, Sanders CT, Mendez BS, De B, et al. AAV2-mediated CLN2 gene transfer to rodent and non-human primate brain results in long-term TPP-I expression compatible with therapy for LINCL. Gene Ther. 2005;12(22):1618-32.
48. Xiao X, Li J, McCown TJ, Samulski RJ. Gene transfer by adeno-associated virus vectors into the central nervous system. Exp Neurol. 1997;144(1):113-24.
49. Hargrove PW, Vanin EF, Kurtzman GJ, Nienhuis AW. High-level globin gene expression mediated by a recombinant adeno-associated virus genome that contains the 3' gamma globin gene regulatory element and integrates as tandem copies in erythroid cells. Blood. 1997;89(6):2167-75.
50. Malik P, McQuiston SA, Yu XJ, Pepper KA, Krall WJ, Podsakoff GM, et al. Recombinant adeno-associated virus mediates a high level of gene transfer but less efficient integration in the K562 human hematopoietic cell line. J Virol. 1997;71(3):1776-83.
51. Nathwani AC, Hanawa H, Vandergriff J, Kelly P, Vanin EF, Nienhuis AW. Efficient gene transfer into human cord blood CD34+ cells and the CD34+CD38- subset using highly purified recombinant adeno-associated viral vector preparations that are free of helper virus and wild-type AAV. Gene Ther. 2000;7(3):183-95.
52. Schuhmann NK, Pozzoli O, Sallach J, Huber A, Avitabile D, Perabo L, et al. Gene transfer into human cord blood-derived CD34(+) cells by adeno-associated viral vectors. Exp Hematol. 2010;38(9):707-17.
53. Veldwijk MR, Sellner L, Stiefelhagen M, Kleinschmidt JA, Laufs S, Topaly J, et al. Pseudotyped recombinant adeno-associated viral vectors mediate efficient gene transfer into primary human CD34(+) peripheral blood progenitor cells. Cytotherapy. 2010;12(1):107-12.
54. Song L, Kauss MA, Kopin E, Chandra M, Ul-Hasan T, Miller E, et al. Optimizing the transduction efficiency of capsid-modified AAV6 serotype vectors in primary human hematopoietic stem cells in vitro and in a xenograft mouse model in vivo. Cytotherapy. 2013;15(8):986-98.
55. Smith LJ, Ul-Hasan T, Carvaines SK, Van Vliet K, Yang E, Wong KK, Jr., et al. Gene transfer properties and structural modeling of human stem cell-derived AAV. Mol Ther. 2014;22(9):1625-34.
56. Wang J, Exline CM, DeClercq JJ, Llewellyn GN, Hayward SB, Li PW, et al. Homology-driven genome editing in hematopoietic stem and progenitor cells using ZFN mRNA and AAV6 donors. Nat Biotech. 2015;33(12):1256-63.
57. Han Z, Zhong L, Maina N, Hu Z, Li X, Chouthai NS, et al. Stable integration of recombinant adeno-associated virus vector genomes after transduction of murine hematopoietic stem cells. Hum Gene Ther. 2008;19(3):267-78.
58. Au-Yeung BB, Shah NH, Shen L, Weiss A. ZAP-70 in Signaling, Biology, and Disease. Annu Rev Immunol. 2018;36:127-56.
59. Lopes N, Vachon H, Marie J, Irla M. Administration of RANKL boosts thymic regeneration upon bone marrow transplantation. EMBO Mol Med. 2017;9(6):835-51.
60. Gillet NA, Malani N, Melamed A, Gormley N, Carter R, Bentley D, et al. The host genomic environment of the provirus determines the abundance of HTLV-1-infected T-cell clones. Blood. 2011;117(11):3113-22.
61. Firouzi S, Lopez Y, Suzuki Y, Nakai K, Sugano S, Yamochi T, et al. Development and validation of a new high-throughput method to investigate the clonality of HTLV-1-infected cells based on provirus integration sites. Genome Med. 2014;6(6):46.
62. Martino AT, Herzog RW, Anegon I, Adjali O. Measuring immune responses to recombinant AAV gene transfer. Methods Mol Biol. 2011;807:259-72.

63. Li QZ, Zhou J, Wandstrat AE, Carr-Johnson F, Branch V, Karp DR, et al. Protein array autoantibody profiles for insights into systemic lupus erythematosus and incomplete lupus syndromes. Clin Exp Immunol. 2007;147(1):60-70.
64. Capo V, Castiello MC, Fontana E, Penna S, Bosticardo M, Draghici E, et al. Efficacy of lentivirus-mediated gene therapy in an Omenn syndrome recombination-activating gene 2 mouse model is not hindered by inflammation and immune dysregulation. J Allergy Clin Immunol. 2017.
65. Rucci F, Poliani PL, Caraffi S, Paganini T, Fontana E, Giliani S, et al. Abnormalities of thymic stroma may contribute to immune dysregulation in murine models of leaky severe combined immunodeficiency. Front Immunol. 2011;2(15).
66. Abramson J, Anderson G. Thymic Epithelial Cells. Annu Rev Immunol. 2017;35:85-118.
67. Anderson MS, Venanzi ES, Klein L, Chen Z, Berzins SP, Turley SJ, et al. Projection of an immunological self shadow within the thymus by the aire protein. Science. 2002;298(5597):1395-401.
68. Lopes N, Serge A, Ferrier P, Irla M. Thymic Crosstalk Coordinates Medulla Organization and T-Cell Tolerance Induction. Front Immunol. 2015;6:365.
69. Abramson J, Goldfarb Y. AIRE: From promiscuous molecular partnerships to promiscuous gene expression. Eur J Immunol. 2016;46(1):22-33.
70. Irla M, Guerri L, Guenot J, Serge A, Lantz O, Liston A, et al. Antigen recognition by autoreactive CD4(+) thymocytes drives homeostasis of the thymic medulla. PLoS One. 2012;7(12):e52591.
71. Gabler J, Arnold J, Kyewski B. Promiscuous gene expression and the developmental dynamics of medullary thymic epithelial cells. Eur J Immunol. 2007;37(12):3363-72.
72. Gray D, Abramson J, Benoist C, Mathis D. Proliferative arrest and rapid turnover of thymic epithelial cells expressing Aire. J Exp Med. 2007;204(11):2521-8.
73. Spangrude GJ, Scollay R. Differentiation of hematopoietic stem cells in irradiated mouse thymic lobes. Kinetics and phenotype of progeny. J Immunol. 1990;145(11):3661-8.
74. Love PE, Bhandoola A. Signal integration and crosstalk during thymocyte migration and emigration. Nat Rev Immunol. 2011;11(7):469-77.
75. McCaughtry TM, Wilken MS, Hogquist KA. Thymic emigration revisited. J Exp Med. 2007;204(11):2513-20.
76. Kimura MY, Thomas J, Tai X, Guinter TI, Shinzawa M, Etzensperger R, et al. Timing and duration of MHC I positive selection signals are adjusted in the thymus to prevent lineage errors. Nat Immunol. 2016;17(12):1415-23.
77. Thomas-Vaslin V, Altes HK, de Boer RJ, Klatzmann D. Comprehensive assessment and mathematical modeling of T cell population dynamics and homeostasis. J Immunol. 2008;180(4):2240-50.
78. Perera J, Huang H. The development and function of thymic B cells. Cell Mol Life Sci. 2015;72(14):2657-63.
79. Perera J, Meng L, Meng F, Huang H. Autoreactive thymic B cells are efficient antigen-presenting cells of cognate self-antigens for T cell negative selection. Proc Natl Acad Sci U S A. 2013;110(42):17011-6.
80. Kumar SR, Markusic DM, Biswas M, High KA, Herzog RW. Clinical development of gene therapy: results and lessons from recent successes. Mol Ther Methods Clin Dev. 2016;3:16034.
81. Colella P, Ronzitti G, Mingozzi F. Emerging Issues in AAV-Mediated In Vivo Gene Therapy. Mol Ther Methods Clin Dev. 2018;8:87-104.
82. Liu X, Adams A, Wildt KF, Aronow B, Feigenbaum L, Bosselut R. Restricting Zap70 expression to CD4+CD8+ thymocytes reveals a T cell receptor-dependent proofreading mechanism controlling the completion of positive selection. J Exp Med. 2003;197(3):363-73.
83. Gascoigne NR, Palmer E. Signaling in thymic selection. Curr Opin Immunol. 2011;23(2):207-12.
84. Singer A, Adoro S, Park JH. Lineage fate and intense debate: myths, models and mechanisms of CD4- versus CD8-lineage choice. Nat Rev Immunol. 2008;8(10):788-801.
85. Etzensperger R, Kadakia T, Tai X, Alag A, Guinter TI, Egawa T, et al. Identification of lineage-specifying cytokines that signal all CD8(+)-cytotoxic-lineage-fate 'decisions' in the thymus. Nat Immunol. 2017;18(11):1218-27.

86. Nowrouzi A, Penaud-Budloo M, Kaeppel C, Appelt U, Le Guiner C, Moullier P, et al. Integration frequency and intermolecular recombination of rAAV vectors in non-human primate skeletal muscle and liver. Mol Ther. 2012;20(6):1177-86.
87. Davis MM, Bjorkman PJ. T-cell antigen receptor genes and T-cell recognition. Nature. 1988;334(6181):395-402.
88. Wang CY, Yu PF, He XB, Fang YX, Cheng WY, Jing ZZ. alphabeta T-cell receptor bias in disease and therapy (Review). Int J Oncol. 2016;48(6):2247-56.
89. Calcedo R, Somanathan S, Qin Q, Betts MR, Rech AJ, Vonderheide RH, et al. Class I-restricted T-cell responses to a polymorphic peptide in a gene therapy clinical trial for alpha-1-antitrypsin deficiency. Proc Natl Acad Sci U S A. 2017;114(7):1655-9.
90. Mingozzi F, High KA. Immune responses to AAV vectors: overcoming barriers to successful gene therapy. Blood. 2013;122(1):23-36.
91. Xiao W, Chirmule N, Schnell MA, Tazelaar J, Hughes JV, Wilson JM. Route of administration determines induction of T-cell-independent humoral responses to adeno-associated virus vectors. Mol Ther. 2000;1(4):323-9.
92. Mendoza SD, El-Shamayleh Y, Horwitz GD. AAV-mediated delivery of optogenetic constructs to the macaque brain triggers humoral immune responses. J Neurophysiol. 2017;117(5):2004-13.
93. Walter JE, Rosen LB, Csomos K, Rosenberg JM, Mathew D, Keszei M, et al. Broad-spectrum antibodies against self-antigens and cytokines in RAG deficiency. J Clin Invest. 2016;126(11):4389.
94. Surh CD, Sprent J. Regulation of mature T cell homeostasis. Semin Immunol. 2005;17(3):183-91.
95. Cowan JE, Parnell SM, Nakamura K, Caamano JH, Lane PJ, Jenkinson EJ, et al. The thymic medulla is required for Foxp3+ regulatory but not conventional CD4+ thymocyte development. J Exp Med. 2013;210(4):675-81.
96. van Ewijk W, Wang B, Hollander G, Kawamoto H, Spanopoulou E, Itoi M, et al. Thymic microenvironments, 3-D versus 2-D? Semin Immunol. 1999;11(1):57-64.
97. Su DM, Navarre S, Oh WJ, Condie BG, Manley NR. A domain of Foxn1 required for crosstalk-dependent thymic epithelial cell differentiation. Nat Immunol. 2003;4(11):1128-35.
98. Dudakov JA, van den Brink MR. Greater than the sum of their parts: combination strategies for immune regeneration following allogeneic hematopoietic stem cell transplantation. Best Pract Res Clin Haematol. 2011;24(3):467-76.
99. Sutherland JS, Goldberg GL, Hammett MV, Uldrich AP, Berzins SP, Heng TS, et al. Activation of thymic regeneration in mice and humans following androgen blockade. J Immunol. 2005;175(4):2741-53.
100. Goldberg GL, Dudakov JA, Reiseger JJ, Seach N, Ueno T, Vlahos K, et al. Sex steroid ablation enhances immune reconstitution following cytotoxic antineoplastic therapy in young mice. J Immunol. 2010;184(11):6014-24.
101. Velardi E, Tsai JJ, Holland AM, Wertheimer T, Yu VW, Zakrzewski JL, et al. Sex steroid blockade enhances thymopoiesis by modulating Notch signaling. J Exp Med. 2014;211(12):2341-9.
102. Min D, Panoskaltsis-Mortari A, Kuro OM, Hollander GA, Blazar BR, Weinberg KI. Sustained thymopoiesis and improvement in functional immunity induced by exogenous KGF administration in murine models of aging. Blood. 2007;109(6):2529-37.
103. Rossi SW, Jeker LT, Ueno T, Kuse S, Keller MP, Zuklys S, et al. Keratinocyte growth factor (KGF) enhances postnatal T-cell development via enhancements in proliferation and function of thymic epithelial cells. Blood. 2007;109(9):3803-11.
104. Dudakov JA, Hanash AM, Jenq RR, Young LF, Ghosh A, Singer NV, et al. Interleukin-22 drives endogenous thymic regeneration in mice. Science. 2012;336(6077):91-5.
105. Reimann C, Six E, Dal-Cortivo L, Schiavo A, Appourchaux K, Lagresle-Peyrou C, et al. Human T-lymphoid progenitors generated in a feeder-cell-free Delta-like-4 culture system promote T-cell reconstitution in NOD/SCID/gammac(-/-) mice. Stem Cells. 2012;30(8):1771-80.
106. Awong G, Singh J, Mohtashami M, Malm M, La Motte-Mohs RN, Benveniste PM, et al. Human proT-cells generated in vitro facilitate hematopoietic stem cell-derived T-lymphopoiesis in vivo and restore thymic architecture. Blood. 2013;122(26):4210-9.
107. Dudakov JA, Mertelsmann AM, O'Connor MH, Jenq RR, Velardi E, Young LF, et al. Loss of thymic innate lymphoid cells leads to impaired thymopoiesis in experimental graft-versus-host disease. Blood. 2017;130(7):933-42.

108. Kelly RM, Goren EM, Taylor PA, Mueller SN, Stefanski HE, Osborn MJ, et al. Short-term inhibition of p53 combined with keratinocyte growth factor improves thymic epithelial cell recovery and enhances T-cell reconstitution after murine bone marrow transplantation. Blood. 2010;115(5):1088-97.
109. Zhang SL, Wang X, Manna S, Zlotoff DA, Bryson JL, Blazar BR, et al. Chemokine treatment rescues profound T-lineage progenitor homing defect after bone marrow transplant conditioning in mice. Blood. 2014.
110. Manna S, Bhandoola A. Intrathymic Injection. Methods Mol Biol. 2016;1323:203-9.
111. Maina N, Han Z, Li X, Hu Z, Zhong L, Bischof D, et al. Recombinant self-complementary adeno-associated virus serotype vector-mediated hematopoietic stem cell transduction and lineage-restricted, long-term transgene expression in a murine serial bone marrow transplantation model. Hum Gene Ther. 2008;19(4):376-83.
112. Ling C, Bhukhai K, Yin Z, Tan M, Yoder MC, Leboulch P, et al. High-Efficiency Transduction of Primary Human Hematopoietic Stem/Progenitor Cells by AAV6 Vectors: Strategies for Overcoming Donor-Variation and Implications in Genome Editing. Scientific reports. 2016;6:35495.
113. Huser D, Khalid D, Lutter T, Hammer EM, Weger S, Hessler M, et al. High Prevalence of Infectious Adeno-associated Virus (AAV) in Human Peripheral Blood Mononuclear Cells Indicative of T Lymphocytes as Sites of AAV Persistence. J Virol. 2017;91(4).
114. Vandamme C, Adjali O, Mingozzi F. Unraveling the Complex Story of Immune Responses to AAV Vectors Trial After Trial. Hum Gene Ther. 2017;28(11):1061-74.
115. Reichel FF, Peters T, Wilhelm B, Biel M, Ueffing M, Wissinger B, et al. Humoral Immune Response After Intravitreal But Not After Subretinal AAV8 in Primates and Patients. Invest Ophthalmol Vis Sci. 2018;59(5):1910-5.
116. Reichel FF, Dauletbekov DL, Klein R, Peters T, Ochakovski GA, Seitz IP, et al. AAV8 Can Induce Innate and Adaptive Immune Response in the Primate Eye. Mol Ther. 2017;25(12):2648-60.
117. McIntosh JH, Cochrane M, Cobbold S, Waldmann H, Nathwani SA, Davidoff AM, et al. Successful attenuation of humoral immunity to viral capsid and transgenic protein following AAV-mediated gene transfer with a non-depleting CD4 antibody and cyclosporine. Gene Ther. 2012;19(1):78-85.
118. Han SO, Li S, Brooks ED, Masat E, Leborgne C, Banugaria S, et al. Enhanced efficacy from gene therapy in Pompe disease using coreceptor blockade. Hum Gene Ther. 2015;26(1):26-35.
119. Corti M, Elder M, Falk D, Lawson L, Smith B, Nayak S, et al. B-Cell Depletion is Protective Against Anti-AAV Capsid Immune Response: A Human Subject Case Study. Mol Ther Methods Clin Dev. 2014;1.
120. Mack DL, Poulard K, Goddard MA, Latournerie V, Snyder JM, Grange RW, et al. Systemic AAV8-Mediated Gene Therapy Drives Whole-Body Correction of Myotubular Myopathy in Dogs. Mol Ther. 2017;25(4):839-54.
121. Elverman M, Goddard MA, Mack D, Snyder JM, Lawlor MW, Meng H, et al. Long-term effects of systemic gene therapy in a canine model of myotubular myopathy. Muscle Nerve. 2017;56(5):943-53.
122. Le Guiner C, Servais L, Montus M, Larcher T, Fraysse B, Moullec S, et al. Long-term microdystrophin gene therapy is effective in a canine model of Duchenne muscular dystrophy. Nat Commun. 2017;8:16105.
123. Mueller C, Chulay JD, Trapnell BC, Humphries M, Carey B, Sandhaus RA, et al. Human Treg responses allow sustained recombinant adeno-associated virus-mediated transgene expression. J Clin Invest. 2013;123(12):5310-8.
124. Gernoux G, Wilson JM, Mueller C. Regulatory and Exhausted T Cell Responses to AAV Capsid. Hum Gene Ther. 2017;28(4):338-49.
125. Foss DL, Donskoy E, Goldschneider I. The importation of hematogenous precursors by the thymus is a gated phenomenon in normal adult mice. J Exp Med. 2001;193(3):365-74.
126. Prockop SE, Petrie HT. Regulation of thymus size by competition for stromal niches among early T cell progenitors. J Immunol. 2004;173(3):1604-11.
127. Adjali O, Vicente RR, Ferrand C, Jacquet C, Mongellaz C, Tiberghien P, et al. Intrathymic administration of hematopoietic progenitor cells enhances T cell reconstitution in ZAP-70 severe combined immunodeficiency. Proc Natl Acad Sci U S A. 2005;102(38):13586-91.

128. de Barros SC, Vicente R, Chebli K, Jacquet C, Zimmermann VS, Taylor N. Intrathymic progenitor cell transplantation across histocompatibility barriers results in the persistence of early thymic progenitors and T-cell differentiation. Blood. 2013;121(11):2144-53.
129. Hirschhorn R, Yang DR, Puck JM, Huie ML, Jiang CK, Kurlandsky LE. Spontaneous in vivo reversion to normal of an inherited mutation in a patient with adenosine deaminase deficiency. Nat Genet. 1996;13(3):290-5.
130. Bousso P, Wahn V, Douagi I, Horneff G, Pannetier C, Le Deist F, et al. Diversity, functionality, and stability of the T cell repertoire derived in vivo from a single human T cell precursor. Proc Natl Acad Sci U S A. 2000;97(1):274-8.
131. Stephan V, Wahn V, Le Deist F, Dirksen U, Broker B, Muller-Fleckenstein I, et al. Atypical X-linked severe combined immunodeficiency due to possible spontaneous reversion of the genetic defect in T cells. N Engl J Med. 1996;335(21):1563-7.
132. Ariga T, Oda N, Yamaguchi K, Kawamura N, Kikuta H, Taniuchi S, et al. T-cell lines from 2 patients with adenosine deaminase (ADA) deficiency showed the restoration of ADA activity resulted from the reversion of an inherited mutation. Blood. 2001;97(9):2896-9.
133. Wada T, Konno A, Schurman SH, Garabedian EK, Anderson SM, Kirby M, et al. Second-site mutation in the Wiskott-Aldrich syndrome (WAS) protein gene causes somatic mosaicism in two WAS siblings. J Clin Invest. 2003;111(9):1389-97.
134. Davis BR, Yan Q, Bui JH, Felix K, Moratto D, Muul LM, et al. Somatic mosaicism in the Wiskott-Aldrich syndrome: molecular and functional characterization of genotypic revertants. Clin Immunol. 2010;135(1):72-83.
135. Davis BR, Dicola MJ, Prokopishyn NL, Rosenberg JB, Moratto D, Muul LM, et al. Unprecedented diversity of genotypic revertants in lymphocytes of a patient with Wiskott-Aldrich syndrome. Blood. 2008;111(10):5064-7.
136. Rieux-Laucat F, Hivroz C, Lim A, Mateo V, Pellier I, Selz F, et al. Inherited and somatic CD3zeta mutations in a patient with T-cell deficiency. N Engl J Med. 2006;354(18):1913-21.
137. Wada T, Toma T, Okamoto H, Kasahara Y, Koizumi S, Agematsu K, et al. Oligoclonal expansion of T lymphocytes with multiple second-site mutations leads to Omenn syndrome in a patient with RAG1-deficient severe combined immunodeficiency. Blood. 2005;106(6):2099-101.
138. Tone Y, Wada T, Shibata F, Toma T, Hashida Y, Kasahara Y, et al. Somatic revertant mosaicism in a patient with leukocyte adhesion deficiency type 1. Blood. 2007;109(3):1182-4.
139. Nishikomori R, Akutagawa H, Maruyama K, Nakata-Hizume M, Ohmori K, Mizuno K, et al. X-linked ectodermal dysplasia and immunodeficiency caused by reversion mosaicism of NEMO reveals a critical role for NEMO in human T-cell development and/or survival. Blood. 2004;103(12):4565-72.
140. Uzel G, Tng E, Rosenzweig SD, Hsu AP, Shaw JM, Horwitz ME, et al. Reversion mutations in patients with leukocyte adhesion deficiency type-1 (LAD-1). Blood. 2008;111(1):209-18.
141. Speckmann C, Pannicke U, Wiech E, Schwarz K, Fisch P, Friedrich W, et al. Clinical and immunologic consequences of a somatic reversion in a patient with X-linked severe combined immunodeficiency. Blood. 2008;112(10):4090-7.

FIGURE LEGENDS

FIG 1. AAV 8, 9 and 10 serotypes efficiently transduce all thymocyte subsets. A, scAAV 8, 9 and 10 serotypes harboring GFP were administered intrathymically (IT) into WT mice and GFP expression was assessed at day 3. Representative CD4/CD8 profiles from non-transduced (grey) and transduced (green) GFP+ thymocytes are presented. **B,** Quantification of the percentages of GFP+ double negative (DN), double positive (DP), single positive CD4 (SP4) and single positive CD8 (SP8) thymocytes are shown and compared to non-transduced WT mice (upper panel). Thymocyte subset repartition within non-transduced (GFP-) and transduced (GFP+) compartments of AAV8-GFP-transduced mice are presented (lower panel; means±SEM). **C,** The percentages of GFP+ thymocytes and lymph node (LN) T cells are presented as a function of time (n=3-5 mice per time point). **D,** Representative plots of GFP- and GFP+ thymocytes at day 3 following IT injection of the scAAV-GFP vector into ZAP-70$^{-/-}$ (KO) mice (left). Quantification of GFP+ cells in KO and AAV-transduced KO mice (n=11) are presented (top). The mean percentages of DN and DP thymocytes within the non-transduced (GFP-, grey) and transduced (GFP+, green) subsets (left bottom panel) as well as the absolute numbers of transduced GFP+ thymocytes are shown (right bottom panel).

FIG 2. Intrathymic AAV8-ZAP-70 gene transfer results in the rapid reconstitution of the thymic architecture in ZAP-70$^{-/-}$ mice. A, ssAAV8-ZAP-70 or scAAV8-GFP virions were IT-injected into ZAP-70$^{-/-}$ (KO) mice and thymi from WT, KO and gene-transduced mice were evaluated for the presence of a thymic medulla by keratin14 (K14) staining and AIRE+ cells. Representative confocal images of thymic tissue sections at 1.5 (10 days), 3 and 10 weeks (w) post gene transfer are shown. **B,** The number of AIRE^{+} cells/mm^2 of thymus were quantified in the indicated conditions. Each point

represents the quantification of individual medulla derived from 3 distinct mice. **C,** Mean percentages of mature SP4 and SP8 thymocytes within the transduced GFP+ and ZAP-70+ subsets are shown in WT (left panel) and ZAP-70$^{-/-}$ (right panel) mice at the indicated time points following intrathymic AAV8-GFP and AAV8-ZAP-70 gene transfer, respectively. **D,** Absolute numbers of SP4 and SP8 thymocytes in WT mice (left panel) and AAV8-ZAP-70-transduced mice (right panel) were determined from the SP4 and SP8 gates at the indicated time points (n=5). Statistical significance was determined using an unpaired 2-tailed t-test or a one-way ANOVA with a Tukey's multiple comparison test; *, $p<0.05$; **, $p<0.01$; ***, $p<0.001$; ****, $p<0.0001$.

FIG 3. Intrathymic AAV8 transduction results in long-term maintenance of peripheral T cells and T lineage-specific transgene expression. **A,** The presence of peripheral blood T cells was monitored by flow cytometry following IT administration of AAV8-GFP or AAV8-ZAP-70 vectors and data from individual mice are presented at 3-43 weeks. Statistical differences between mice treated by IT AAV8-ZAP-70 gene transfer as compared to IT AAV8-GFP transfer or control KO mice were evaluated by a one-way ANOVA with a Tukey's multiple comparison test for the following time groups; 3-10 weeks, 11-20 weeks, 21-30 weeks and 31-40 weeks (***, $p<0.001$, for all groups). **B,** The percentages of peripheral CD4+, CD8+, CD19+ and CD11b+ hematopoietic cells expressing ectopic ZAP-70 following IT AAV8-ZAP-70 transduction are presented. **C,** ZAP-70 protein expression in transduced T cells was evaluated by intracellular staining and MFI relative to WT T cells are presented at the indicated time points. **D,** Representative plots of CD3+ lymph node T cells are presented. Total T cell numbers (means±SEM) are shown (right). **E,** The repartition of CD4/CD8 lymphocytes and mean CD4/CD8 ratios are shown at the indicated time points. Statistical significance was determined by a 2-tailed unpaired t-test *, $p<0.05$.

FIG 4. AAV8-ZAP-70-transduced peripheral T lymphocytes exhibit stable vector genomes following TCR-induced proliferation and diverse TCR repertoires. A, AAV genome copy number in lymph node samples was assessed by qPCR in IT AAV8-ZAP-70-transduced mice at the indicated time points. Vector genomes per diploid genome (Vg/Dg) were quantified relative to the albumin gene and normalized to the percentage of T cells. **B,** Proliferation was assessed following TCR stimulation by CTV fluorescence and representative histograms at day 0 (light grey) and day 4 (dark grey) are shown. AAV genome copy was monitored as above and quantifications (n=9) are shown (p, non-significant (ns)). **C**, Schematic representation of the AAV-ZAP-70 vector are shown. PCR products, representing integrated vector, are shown at the indicated time points and T cells from WT mice are presented as a negative control. **D**, The number of distinct TRA V, TRA J, TRA VJ, TRB V, TRB J, TRB VJ, TRA and TRB clonotypes are presented (top). Clonotype frequencies are presented with each clonotype represented by a dot whose size is proportional to its frequency. Violin plots represent the density of the distribution and black dots show the median frequency per repertoire (bottom).

FIG 5. Induction of a T cell-independent humoral response to AAV8 capsid epitopes following intrathymic vector administration. A, Total IgG titers against OVA were monitored in non-immunized WT, KO and IT-AAV8-ZAP-70-treated KO mice (46w post gene transfer) and 6 weeks post immunization by ELISA. Reactivity was monitored as a function of dilution, as indicated (n=4). Statistical significance was evaluated at each dilution by a one-way ANOVA with a Tukey's multiple comparison test for each dilution and is noted for significant differences; ***, $p<0.001$; **, $p<0.01$. **B,** Neutralizing antibodies (Nab) against the AAV8 serotype was monitored in WT and ZAP-$70^{-/-}$ mice following intrathymic AAV8-GFP and AAV8-ZAP-70 transduction. Serum

dilutions of 1:10, 1:100 and 1:1000 are shown by the decreasing slope of the triangle, respectively, and Nab activity is defined as a decrease in AAV transduction of >50% compared to AAV incubation with PBS alone (red line). Each point represents serum from an individual mouse at 3, 10 and 17 weeks post transduction and mean levels are indicated by a horizontal line. **C,** Antibodies against ZAP-70 protein were measured by ELISA and data are presented as ng of antibody/ ml of serum. Antibody levels of >25ng/ml are considered significant.

FIG 6. Transient induction of a broad spectrum of antibodies in ZAP-70$^{-/-}$ mice following intrathymic AAV8 gene transfer remains significantly lower than that detected in autoimmune mice. A, The presence of IgG autoantibodies in serum samples of ZAP-70$^{-/-}$ (KO) mice and following IT administration of either AAV8-GFP or AAV8-ZAP-70 vectors was evaluated at the indicated time points. IgG autoantibodies against 123 antigens were assessed by protein microarray and heat maps showing autoantibody reactivity relative to levels in age-matched WT mice are presented. **B,** The levels of auto-antibodies against RNP, dsDNA and SSA were evaluated by ELISA in control MRL/MpJ mice, autoimmune-prone MRL/*lpr* mice and IT:AAV8-ZAP-70-treated mice at 10 and 43 weeks post gene transfer. Each point represents serum from an individual mouse and statistical significance was determined by a one-way ANOVA with a Tukey's multiple comparison test and significance is indicated; **, $p<0.01$; ***, $p<0.001$ ****, $p<0.0001$, ns-non significant.

FIG 7. AAV8-ZAP-70-transduced thymocytes differentiate into effector and regulatory T cells. A, The presence of naïve (CD62L+CD44-, N), central memory (CD62L+ CD44+, CM), and effector memory (CD62L-CD44+, EM) cells within the CD4 and CD8 subsets were monitored at 3, 10, 17 and 43 weeks post IT-AAV8-ZAP-70 gene transfer. The percentages of cells in each

subset were quantified at each time point and mean levels ± SEM (n=4-5 mice per time point) are presented. **B,** LN cells from the indicated mice were stimulated *ex vivo* with anti-CD3/anti-CD28 mAbs for 3 days and cytokine secretion was measured. Each point represents data from a single mouse and horizontal lines represent mean levels (pg/ml). **C,** The percentages of Foxp3+CD25+ peripheral Tregs was evaluated and representative dot plots are presented (left) together with mean percentages ± SEM at each time point (n=5-14 mice per time point, right). **D,** Conventional and regulatory CD4 T cell subsets were FACS-sorted on the basis of CD25 expression. Foxp3 and IL-10 transcripts in each subset were monitored by qRT-PCR (n=2 to 4 mice in 2 independent experiments). Statistical significance was determined by a 2-tailed unpaired t-test and significance is indicated; *, $p<0.05$; **, $p<0.01$; ***, $p<0.001$ ****, $p<0.0001$.

Online Repository

MATERIALS AND METHODS

rAAV constructs and vector production. The human ZAP-70 gene was cloned downstream of the murine phosphoglycerate kinase (PGK) promoter with the bovine growth hormone (BGH) polyadenylation signal sequences flanked by two AAV2-ITRs sequences. For the green fluorescent protein (GFP) coding vector plasmid, the PGK promoter is upstream of the GFP sequence and the simian virus 40 (SV40) polyadenylation signal.

Self-complementary (sc) AAV-8, AAV-9 and AAV-10 harboring GFP and single-stranded (ss) AAV-8 harboring ZAP-70 vector stocks were produced by cotransfection of HEK293 cells with the vector plasmid and the pDG plasmid[1], an adenoviral plasmid providing helper functions needed for rAAV assembly, as previously described[2]. Supernatants were precipitated with polyethylene glycol (PEG, Sigma-Aldrich) and resuspended in TBS before benzonase digestion. Vector-containing supernatants were purified on a double CsCl gradient with the first gradient centrifuged at 28,000 rpm for 24 hours at 15°C and the band harboring full particles was centrifuged at 38,000 rpm for 48 hours. Viral suspensions were then subjected to 4 successive rounds of dialysis against DPBS in a Slide-a Lyzer cassette (Thermo Scientific). The number of infectious particles/ml in the purified vector prep was determined using a stable rep-cap HeLa cell line in a modified Replication Center Assay (RCA)[3]. Vectors were stored at <-70°C in polypropylene low-binding cryovials.

Mice and intrathymic AAV gene therapy. C57Bl/6 mice ZAP-70$^{-/-}$ mice were maintained under specific pathogen-free conditions in the IGMM animal facility (Montpellier, France). Serum from female MRL/lpr and sex-matched control

MRL/MpJ mice were generously provided by Luz Blanco and Mariana Kaplan (NIAMS, NIH). Intrathymic injections were performed in 2.5-3 week old non-conditioned mice with rAAV vectors (1-3x10^{13} vg/kg) as previously described[4]. Briefly, non-conditioned mice were anesthetized with isoflurane and vectors were directly injected into the thymus (20 μl total volume) by insertion of a 0.3 ml 28 gauge 8 mm insulin syringe through the skin into the thoracic cavity above the sternum. All experiments were approved by the local animal facility institutional review board in accordance with national guidelines.

Immunophenotyping, T cell activations and flow cytometry analyses. Cells, isolated from thymi, lymph nodes or spleen, were stained with the appropriate conjugated αCD3, αCD4, αCD8, αCD11b, αCD19, αCD25, αCD62L, αCD39, αCD44 αCTLA4 and αGITR mAbs (Becton Dickinson, San Diego, CA). Intracellular staining for Foxp3 and ZAP-70 was performed following fixation/permeabilization (eBioscience) and using the BD Biosciences kit, respectively. Cell activations were performed using plate-bound anti-CD3 (clone 17A2; 1 μg/ml) and anti-CD28 (clone PV-1; 1 μg/ml) mAbs in RPMI 1640 media (Life Technologies) supplemented with 10% FCS. Cell proliferation was monitored by labelling with CTV (Life Technologies; 5 μM) for 3 min at RT. Cytokine production was monitored using a Cytometric Bead Array (CBA) Kit (BD Biosciences). Stained cells were analyzed by flow cytometry (FACS-Canto II or LSR II-Fortessa, Becton Dickinson, San Jose, CA). Data analyses were performed using Diva (BD Biosciences), FlowJo Mac v.10.4.2 software (Tree Star) and FCAP Array Software (CBA analysis).

Immunohistochemistry. Frozen thymic sections were stained as previously described[5]. Sections were stained with anti-keratin 14 (1:800; AF64, Covance Research) and a secondary Cy3-conjugated anti-rabbit (1:500; Invitrogen) Ab

together with an Alexa Fluor 488-conjugated anti-AIRE mAb (1:200; 5H12, eBioscience). They were then counterstained with 1 ug/ml DAPI as reported[6]. Images were acquired on a LSM 780 Zeiss and SP5 Leica confocal microscopes and quantified using ImageJ and Matlab software.

Quantitative real-time PCR for evaluation of vector genomes and qRT-PCR for cellular genes. Total DNA was extracted using the Gentra Puregene kit (Qiagen) and Tissue Lyser II (Qiagen) according to the manufacturer's instructions. Vector genome DNAs were measured through quantification of BGH-pA by quantitative PCR with Premix Ex Taq kit (Takara). Primers were: 5'-TCTAGTTGCCAGCCATCTGTTGT-3' (forward) and 5'-TGGGAGTGGCACCTTCCA-3' (reverse) and the BGH-pA TaqMan probe was: 5'-(6 FAM)-TCCCCCGTGCCTTCCTTGACC-(TAMRA)-3'. Primers for endogenous albumin were: 5'-ACATAGCTTGCTTCAGAACGGT-3' (forward) and 5'-AGTGTCTTCATCCTGCCCTAAA-3' (reverse). Quantitative PCR for BGH-pA was performed using the following program: initial denaturation 20 sec at 95°C followed by 45 cycles of 1 sec at 95°C and 20 sec at 60°C. qPCR for albumin was performed as follows: initial denaturation for 20 sec at 95°C followed by 45 cycles of 3 sec at 90°C and 30 sec at 60°C. For each qPCR, cycle threshold values (Ct) were compared with those obtained using dilutions of plasmids harboring either the BGH-pA or albumin genes and results are expressed as vector genome per diploid genome (vg/dg).

For assessment of IL-10 and Foxp3 mRNA levels, $CD4^+CD25^-$ and $CD4^+CD25^{Hi}$ cells from WT and IT:AAV8-ZAP-70 mice (15 weeks post-injection) were sorted on a FACSAria and RNA extraction was performed using the RNeasy Mini kit (Qiagen). RNA was reverse-transcribed into cDNA by oligonucleotide priming using the QuantiTect Reverse Transcription Kit (Qiagen). Each sample was amplified in triplicate (LightCycler 480, Roche) and

normalized to HPRT levels using the following specific primers: Foxp3-sense: 5'-GGCCCTTCTCCAGGACAGA-3', Foxp3-antisense: 5′-GCTGATCATGGCTGGGTTGT-3′, IL10-sense: 5'-AACTGCTCCACTGCCTTGCT-3', IL10-antisense: 5'-GGTTGCCAAGCCTTATCGGA-3' Hprt-sense: 5′-CTGGTGAA-AAGGACCTCTCG-3′, Hprt-antisense: 5′-TGAAGTACTCATTATAGTCAAGGGCA-3′.

Vector integration analysis. To assess AAV integration, we adopted a sonication-based linker-mediated PCR method, as previously described [7, 8]. Briefly, genomic DNA was sheared using a Covaris E220 Ultrasonicator (Covaris Inc.), generating fragments with a target size of 1,000 bp. The fragmented DNA was subjected to end repair, 3' adenylation and ligation (NEBNext® Ultra™ DNA Library Prep Kit for Illumina®, New England Biolabs) to custom linker cassettes (LC) (Integrated DNA Technologies). LC sequences contain: i) 8 nucleotides barcode, used for sample identification and ii) 12 random nucleotides, used for quantification purposes. Ligation products were subjected to 35 cycles of exponential PCR with primers complementary to 8 different regions of the AAV genome (see Fig 4, C and primers available upon request), and the LC. For each set of AAV-specific primers, the procedure was performed in technical replicates (n=2-3) starting from 5 to 120 ng of sheared DNA. All final PCR products were quantified by qPCR using the Kapa Biosystems Library Quantification Kit for Illumina, following the manufacturer's instructions. qPCR was performed in triplicate on each PCR product diluted 10^{-3}, and the concentrations were calculated by plotting the average Ct values against the provided standard curve, using absolute quantification.

TCR Deep Sequencing and Data Processing. Cells from lymph nodes were pooled, lysed and RNAs extracted**.** T cell receptor (TCR) alpha/beta libraries

were prepared with 100 ng of total RNA from each sample using the SMARTer Mouse TCR α/β Profiling Kit from Takarabio® and sequenced by MiSeq V3 2x300bp (Illumina®). Raw data were aligned and curated using the MiXCR software (v2.1.10)[9]. Alpha and Beta chains were analyzed together. Each sample was defined as a combination of TRV-CDR3aa-TRJ sequences and their associated counts. For representation and analyses, datasets were normalized by a sampling step. The sampling size was equal to the smallest sequence number observed in the analyzed samples (n=687). The sampling was performed for each dataset by 100 random draws of sequences and unique TCRs were listed and counted. Analyses and figures were executed and created using R Studio (version 3.5.0).

Evaluation of humoral immune responses. For evaluation of *in vivo* T cell responses, WT and AAV8-reconstituted mice (46w post gene transfer, 49 weeks of age) were immunized with ovalbumin (3x200 μg complexed with complete Freund's adjuvant at Day 0, incomplete Freund's adjuvant at day 14 and LPS at day 28). Serum IgG levels were evaluated at time 0 and 6 weeks post immunization by enzyme-linked immunosorbent assay (ELISA). Serum anti-ZAP-70 antibodies were evaluated by ELISA at different time points post gene transfer. Briefly, 96 well plates (Nunc MaxiSorp, Thermo Scientific) were coated with recombinant ZAP-70 protein (0.5 µg/mL, Thermo Scientific), sera were added at 1:100 and 1:500 dilutions and a standard scale was generated by serial dilutions of an anti-ZAP-70 mAb (clone 1E7.2, Thermo Scientific). Responsiveness was monitored by horseradish peroxidase-conjugated goat anti-mouse IgG (Dako) and revealed using 2.2-3,3',5,5'-Tetramethylbenzidine (TMB, BD OptEIA, BD Biosciences). The threshold of positivity was determined by averaging the signal of 23 negative sera obtained from naive or AAV GFP injected mice $\pm$ 2*SD. Serum anti-double stranded DNA (dsDNA), anti-ribonucleoprotein (RNP) and SSA (Sjögren's-syndrome-related antigen A)

were quantified by ELISA following the manufacturer's instructions (Alpha Diagnostic International, San Antonio, TX).

The presence of neutralizing antibody in serum samples was monitored as previously described[10]. Two hours prior to rAAV infection, a permissive cell line was infected with wild-type Adenovirus serotype 5. During this incubation time, a rAAV2/8 expressing the reporter gene LacZ (encoding beta-galactosidase) was incubated with serial dilutions of serum and the mix was added to the cell line. Infection was assessed using the luminescent β-galactosidase substrate (Tropix Galacto-Star kit, Thermo Scientific) at 48h. The neutralizing capacity of a given serum is expressed as the titer corresponding to the highest serum dilution at which more than 50% of maximal infection is inhibited.

Screening for IgM and IgG reactivity against 123 autoantigens was performed using autoantibody arrays (UT Southwestern Medical Center, Genomic and Microarray Core Facility, Dallas, Texas) as previously described[11, 12] and heatmaps were generated using R software.

Statistical analyses

Data were analyzed using GraphPad software version 5 and 8 (Graph Pad Prism, La Jolla, CA) and p values were calculated using unpaired t-tests, one-way ANOVA (Tukey's multiple comparison test), and Mann-Whitney tests, as indicated. P values for comparisons of all conditions in the different figure panels are presented in the figure legends.

Extended Figures

Fig E1. Intrathymic AAV8-ZAP-70 gene transfer results in alterations in medulla area in ZAP-70$^{-/-}$ mice. A, Thymic medulla area was evaluated by keratin14 (K14) staining. Representative confocal images of thymic tissue

sections are presented in Figure 2. Quantification of the medullary area in mm^2 of thymus was quantified in the indicated conditions. Each point represents the quantification of individual medulla derived from 2-3 mice at the indicated time points and significance was determined by a 2-tailed unpaired t-test. ns, non-significant; **, p<0.01; ****, p<0.0001. **B,** The absolute numbers of thymocytes in IT-AAV8-ZAP-70 transduced KO mice (n=11) were determined at 3 weeks post gene transfer as well as in age-matched WT and KO control mice (n=3-10). Each point represents an individual mouse with horizontal lines showing means. Data between groups were not significantly different.

Fig E2. Transient induction of a broad spectrum of IgM antibodies in ZAP-$70^{-/-}$ mice following intrathymic AAV8 gene transfer. IgM autoantibody levels were evaluated in sera of ZAP-$70^{-/-}$ (KO) mice and following IT administration of either AAV8-GFP or AAV8-ZAP-70 vectors at the indicated time points. IgM autoantibodies against 123 antigens were assessed by protein microarray. Heat maps showing autoantibody reactivity relative to levels in age-matched WT mice are presented.

Fig E3. High expression of Treg markers in IT: AAV8-ZAP-70-transduced mice. A, Cytokine levels in sera of WT and ZAP-$70^{-/-}$ mice treated by IT AAV8-ZAP-70 gene transfer was evaluated at 3, 10, and 43 weeks post injection by cytokine bead array. Each point represents data from a single mouse and horizontal lines represent mean levels (pg/ml). Statistical significance was determined by a 2-tailed Mann-Whitney test and no groups exhibited significant differences. **B,** Surface levels of CTLA4, GITR and CD39 on $CD4^+CD25^{Hi}$ T cells from WT and IT:AAV8-ZAP-70-transduced KO mice were evaluated by flow cytometry and representative histograms are shown (top). Quantification of the mean fluorescence intensity (MFI) in T cells from individual mice are

presented and significance was assessed by an unpaired t-test (bottom). **, $p<0.01$; ****, $p<0.0001$

References

1. Grimm D, Kay MA, Kleinschmidt JA. Helper virus-free, optically controllable, and two-plasmid-based production of adeno-associated virus vectors of serotypes 1 to 6. Mol Ther. 2003;7(6):839-50.
2. Chenuaud P, Larcher T, Rabinowitz JE, Provost N, Joussemet B, Bujard H, et al. Optimal design of a single recombinant adeno-associated virus derived from serotypes 1 and 2 to achieve more tightly regulated transgene expression from nonhuman primate muscle. Mol Ther. 2004;9(3):410-8.
3. Salvetti A, Oreve S, Chadeuf G, Favre D, Cherel Y, Champion-Arnaud P, et al. Factors influencing recombinant adeno-associated virus production. Hum Gene Ther. 1998;9(5):695-706.
4. Vicente R, Adjali O, Jacquet C, Zimmermann VS, Taylor N. Intrathymic transplantation of bone marrow-derived progenitors provides long-term thymopoiesis. Blood. 2010;115(10):1913-20.
5. Lopes N, Vachon H, Marie J, Irla M. Administration of RANKL boosts thymic regeneration upon bone marrow transplantation. EMBO Mol Med. 2017;9(6):835-51.
6. Serge A, Bailly AL, Aurrand-Lions M, Imhof BA, Irla M. For3D: Full organ reconstruction in 3D, an automatized tool for deciphering the complexity of lymphoid organs. Journal of immunological methods. 2015;424:32-42.
7. Firouzi S, Lopez Y, Suzuki Y, Nakai K, Sugano S, Yamochi T, et al. Development and validation of a new high-throughput method to investigate the clonality of HTLV-1-infected cells based on provirus integration sites. Genome Med. 2014;6(6):46.
8. Gillet NA, Malani N, Melamed A, Gormley N, Carter R, Bentley D, et al. The host genomic environment of the provirus determines the abundance of HTLV-1-infected T-cell clones. Blood. 2011;117(11):3113-22.
9. Bolotin DA, Poslavsky S, Mitrophanov I, Shugay M, Mamedov IZ, Putintseva EV, et al. MiXCR: software for comprehensive adaptive immunity profiling. Nat Methods. 2015;12(5):380-1.
10. Martino AT, Herzog RW, Anegon I, Adjali O. Measuring immune responses to recombinant AAV gene transfer. Methods Mol Biol. 2011;807:259-72.
11. Li QZ, Zhou J, Wandstrat AE, Carr-Johnson F, Branch V, Karp DR, et al. Protein array autoantibody profiles for insights into systemic lupus erythematosus and incomplete lupus syndromes. Clin Exp Immunol. 2007;147(1):60-70.
12. Capo V, Castiello MC, Fontana E, Penna S, Bosticardo M, Draghici E, et al. Efficacy of lentivirus-mediated gene therapy in an Omenn syndrome recombination-activating gene 2 mouse model is not hindered by inflammation and immune dysregulation. J Allergy Clin Immunol. 2018;142(3):928-41 e8.

Fig 1

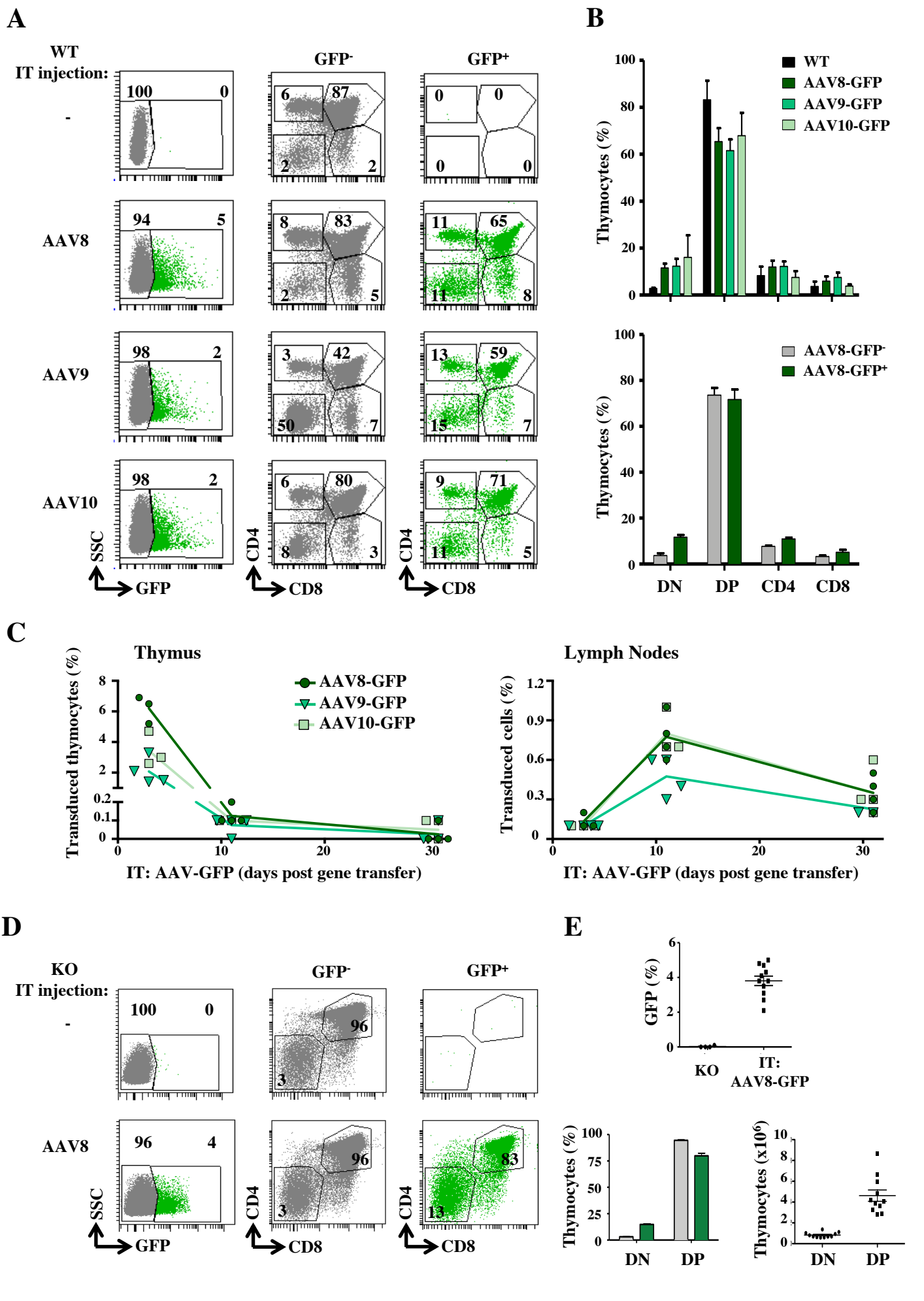
A
WT
IT injection:
-
AAV8
AAV9
AAV10
GFP-
GFP+
100
0
6
87
2
2
0
0
0
0
94
5
8
83
2
5
11
65
11
8
98
2
3
42
50
7
13
59
15
7
98
2
6
80
8
3
9
71
11
5
SSC
GFP
CD4
CD8
CD4
CD8
B
WT
AAV8-GFP
AAV9-GFP
AAV10-GFP
Thymocytes (%)
AAV8-GFP-
AAV8-GFP+
DN
DP
CD4
CD8
C
Thymus
Lymph Nodes
AAV8-GFP
AAV9-GFP
AAV10-GFP
Transduced thymocytes (%)
Transduced cells (%)
IT: AAV-GFP (days post gene transfer)
IT: AAV-GFP (days post gene transfer)
D
KO
IT injection:
-
AAV8
GFP-
GFP+
100
0
96
3
96
4
96
3
83
13
SSC
GFP
CD4
CD8
CD4
CD8
E
GFP (%)
KO
IT:
AAV8-GFP
Thymocytes (%)
DN
DP
Thymocytes (x10^6)
DN
DP

Fig 2

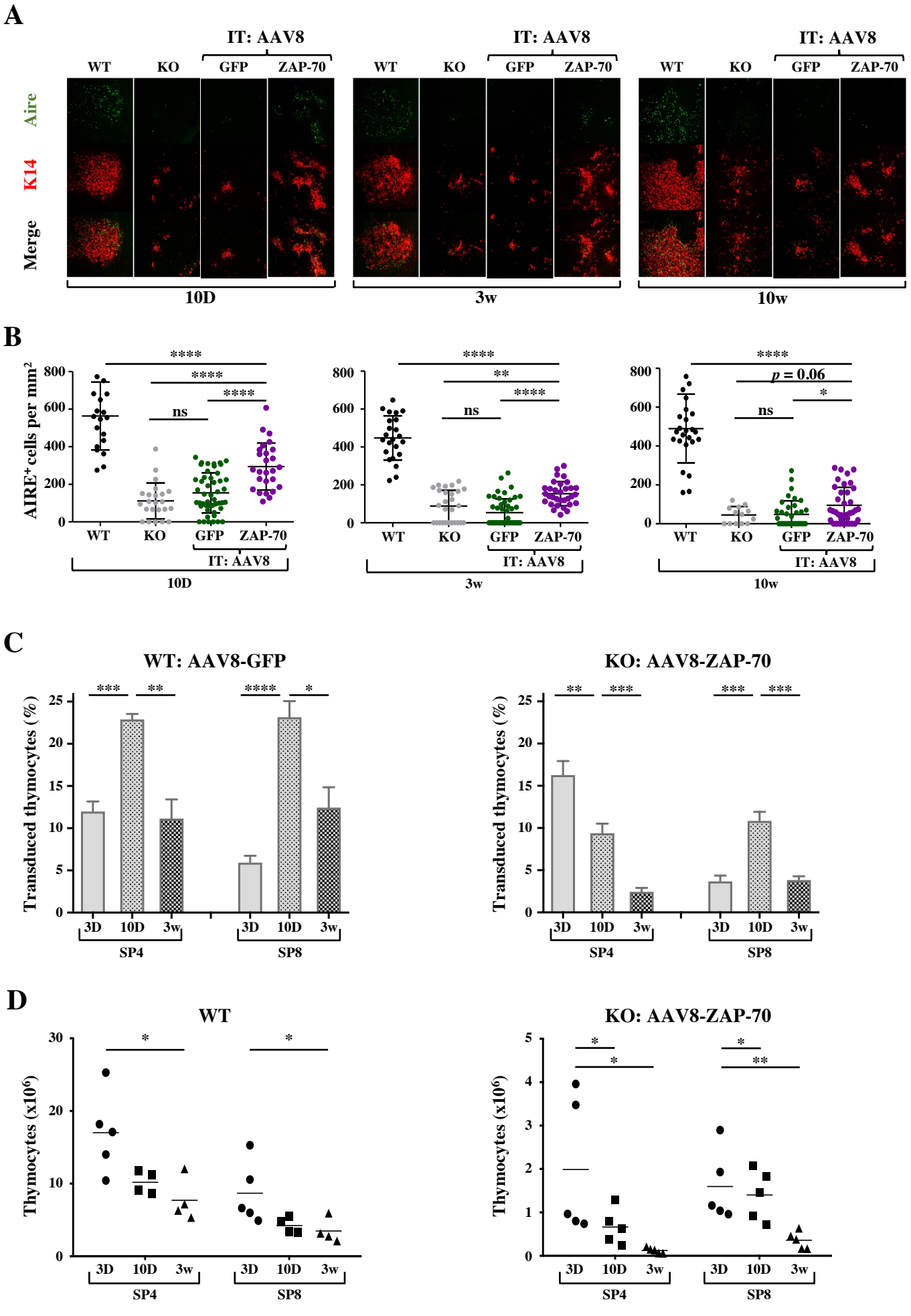
A
IT: AAV8
WT
KO
GFP
ZAP-70
Aire
K14
Merge
10D
3w
10w
B
AIRE+ cells per mm2
****
**
ns
p = 0.06
*
C
WT: AAV8-GFP
KO: AAV8-ZAP-70
Transduced thymocytes (%)
***
3D
10D
3w
SP4
SP8
D
WT
KO: AAV8-ZAP-70
Thymocytes (x10^6)

Fig 3

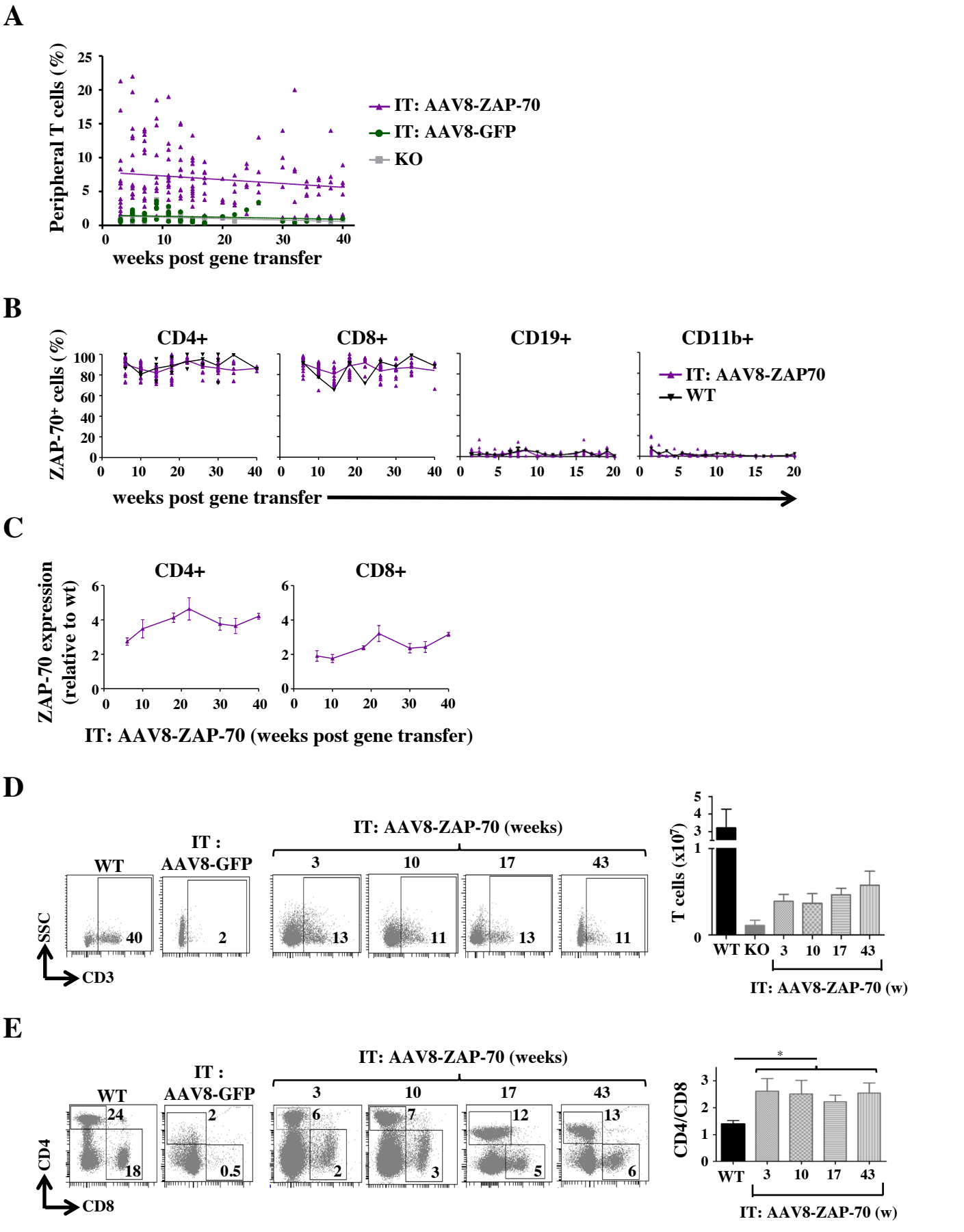
A
Peripheral T cells (%)
weeks post gene transfer
IT: AAV8-ZAP-70
IT: AAV8-GFP
KO
B
CD4+
CD8+
CD19+
CD11b+
ZAP-70+ cells (%)
IT: AAV8-ZAP70
WT
weeks post gene transfer
C
CD4+
CD8+
ZAP-70 expression (relative to wt)
IT: AAV8-ZAP-70 (weeks post gene transfer)
D
WT
IT : AAV8-GFP
IT: AAV8-ZAP-70 (weeks)
3
10
17
43
SSC
CD3
40
2
13
11
13
11
T cells (x10^7)
WT KO 3 10 17 43
IT: AAV8-ZAP-70 (w)
E
WT
IT : AAV8-GFP
IT: AAV8-ZAP-70 (weeks)
3
10
17
43
CD4
CD8
24
18
2
0.5
6
2
7
3
12
5
13
6
CD4/CD8
WT 3 10 17 43
IT: AAV8-ZAP-70 (w)

Fig 4

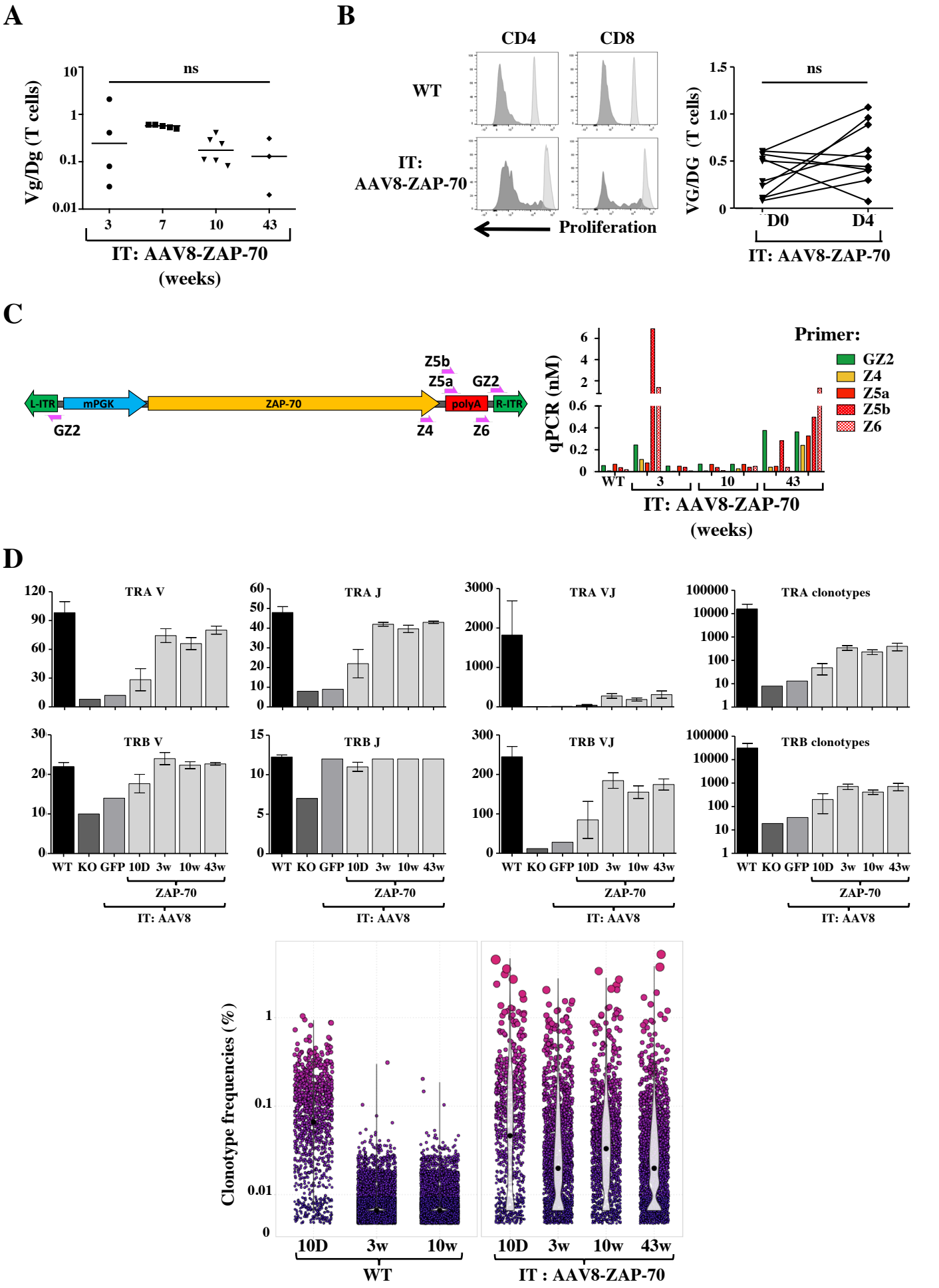
A
Vg/Dg (T cells)
ns
3
7
10
43
IT: AAV8-ZAP-70
(weeks)
B
CD4
CD8
WT
IT:
AAV8-ZAP-70
Proliferation
VG/DG (T cells)
ns
D0
D4
IT: AAV8-ZAP-70
C
L-ITR
mPGK
ZAP-70
polyA
R-ITR
GZ2
Z5b
Z5a
GZ2
Z4
Z6
qPCR (nM)
Primer:
GZ2
Z4
Z5a
Z5b
Z6
WT
3
10
43
IT: AAV8-ZAP-70
(weeks)
D
TRA V
TRA J
TRA VJ
TRA clonotypes
TRB V
TRB J
TRB VJ
TRB clonotypes
WT KO GFP 10D 3w 10w 43w
ZAP-70
IT: AAV8
Clonotype frequencies (%)
10D
3w
10w
WT
10D
3w
10w
43w
IT : AAV8-ZAP-70

Fig 5

A

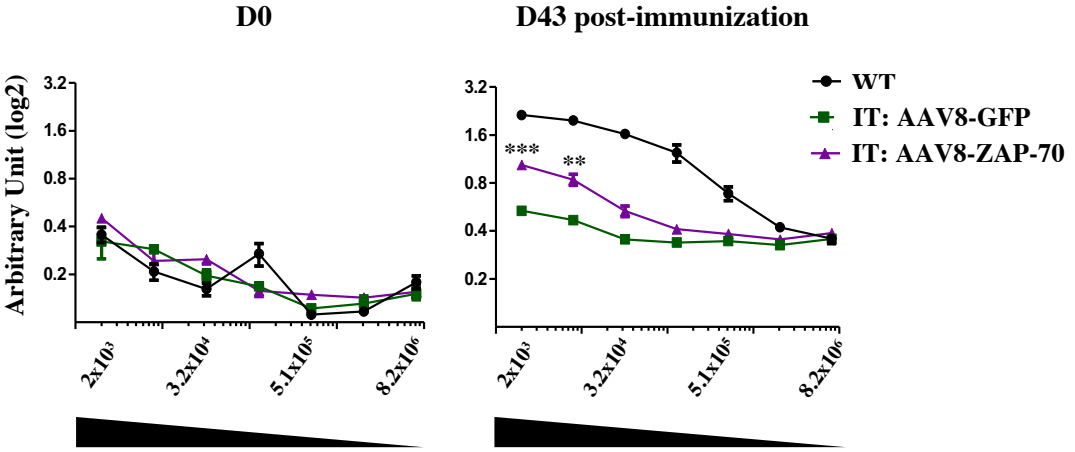
D0
D43 post-immunization
Arbitrary Unit (log2)
3.2
1.6
0.8
0.4
0.2
2x10³
3.2x10⁴
5.1x10⁵
8.2x10⁶
***
**
WT
IT: AAV8-GFP
IT: AAV8-ZAP-70

B

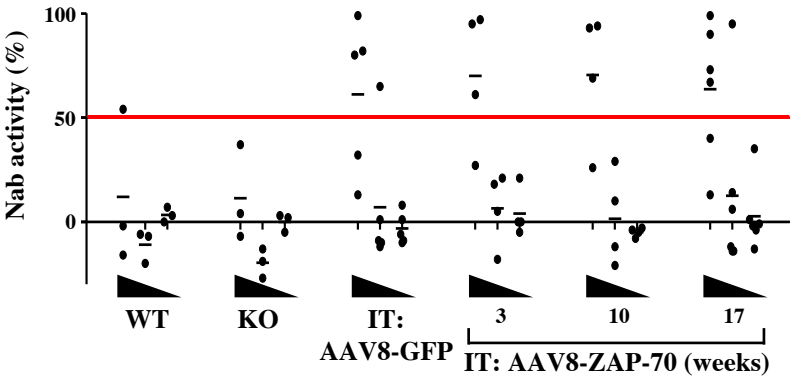
Nab activity (%)
100
50
0
WT
KO
IT: AAV8-GFP
3
10
17
IT: AAV8-ZAP-70 (weeks)

C

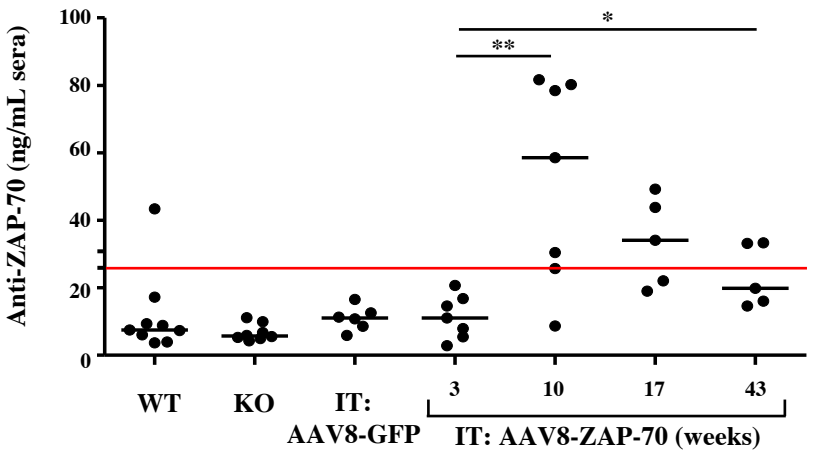
Anti-ZAP-70 (ng/mL sera)
100
80
60
40
20
0
*
**
WT
KO
IT: AAV8-GFP
3
10
17
43
IT: AAV8-ZAP-70 (weeks)

Fig 6

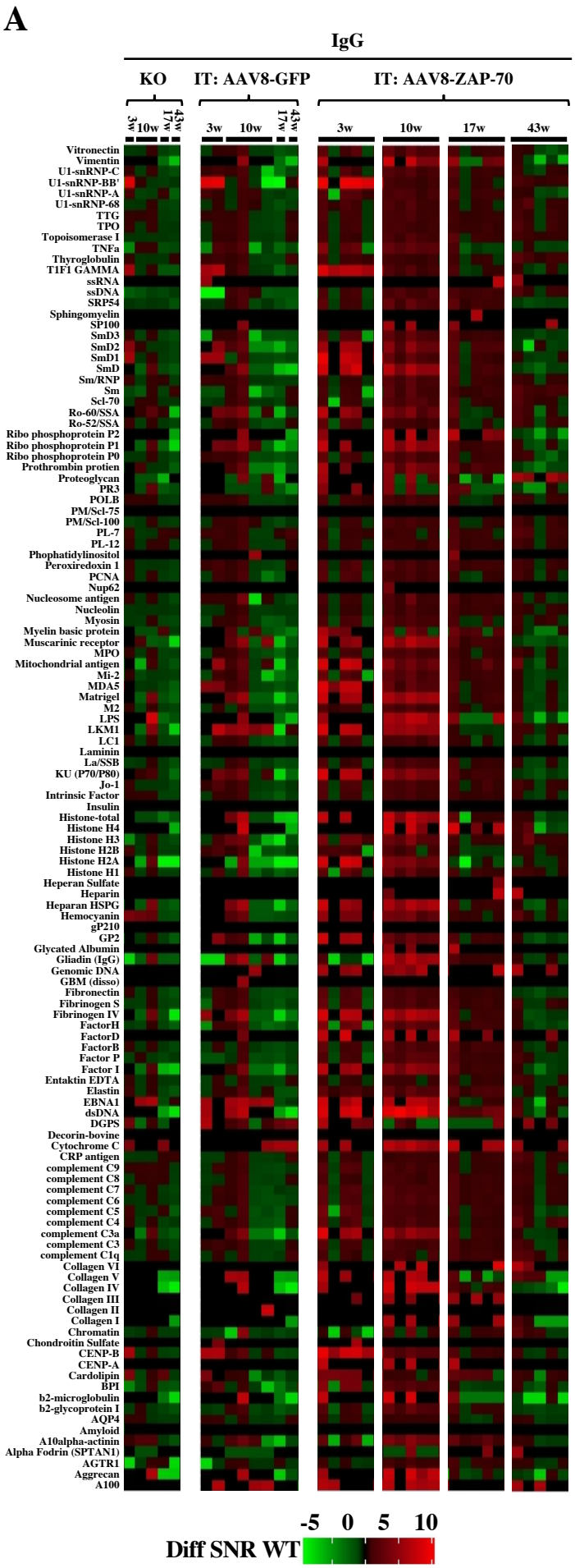
A
IgG
KO
IT: AAV8-GFP
IT: AAV8-ZAP-70
3w
10w
17w
43w
Vitronectin
Vimentin
U1-snRNP-C
U1-snRNP-BB'
U1-snRNP-A
U1-snRNP-68
TTG
TPO
Topoisomerase I
TNFa
Thyroglobulin
T1F1 GAMMA
ssRNA
ssDNA
SRP54
Sphingomyelin
SP100
SmD3
SmD2
SmD1
SmD
Sm/RNP
Sm
Scl-70
Ro-60/SSA
Ro-52/SSA
Ribo phosphoprotein P2
Ribo phosphoprotein P1
Ribo phosphoprotein P0
Prothrombin protien
Proteoglycan
PR3
POLB
PM/Scl-75
PM/Scl-100
PL-7
PL-12
Phophatidylinositol
Peroxiredoxin 1
PCNA
Nup62
Nucleosome antigen
Nucleolin
Myosin
Myelin basic protein
Muscarinic receptor
MPO
Mitochondrial antigen
Mi-2
MDA5
Matrigel
M2
LPS
LKM1
LC1
Laminin
La/SSB
KU (P70/P80)
Jo-1
Intrinsic Factor
Insulin
Histone-total
Histone H4
Histone H3
Histone H2B
Histone H2A
Histone H1
Heperan Sulfate
Heparin
Heparan HSPG
Hemocyanin
gP210
GP2
Glycated Albumin
Gliadin (IgG)
Genomic DNA
GBM (disso)
Fibronectin
Fibrinogen S
Fibrinogen IV
FactorH
FactorD
FactorB
Factor P
Factor I
Entaktin EDTA
Elastin
EBNA1
dsDNA
DGPS
Decorin-bovine
Cytochrome C
CRP antigen
complement C9
complement C8
complement C7
complement C6
complement C5
complement C4
complement C3a
complement C3
complement C1q
Collagen VI
Collagen V
Collagen IV
Collagen III
Collagen II
Collagen I
Chromatin
Chondroitin Sulfate
CENP-B
CENP-A
Cardolipin
BPI
b2-microglobulin
b2-glycoprotein I
AQP4
Amyloid
A10alpha-actinin
Alpha Fodrin (SPTAN1)
AGTR1
Aggrecan
A100
-5
0
5
10
Diff SNR WT
B
α-dsDNA (x10³ U/mL)
600
400
200
0
****
****
****
ns
α-RNP (x10³ U/mL)
15
10
5
0
***
**
***
ns
α-SSA (x10³ U/mL)
8
6
4
2
0
****
***
***
ns
CTRL
MRL/lpr
10w
43w
IT: AAV8-ZAP-70

Fig 7

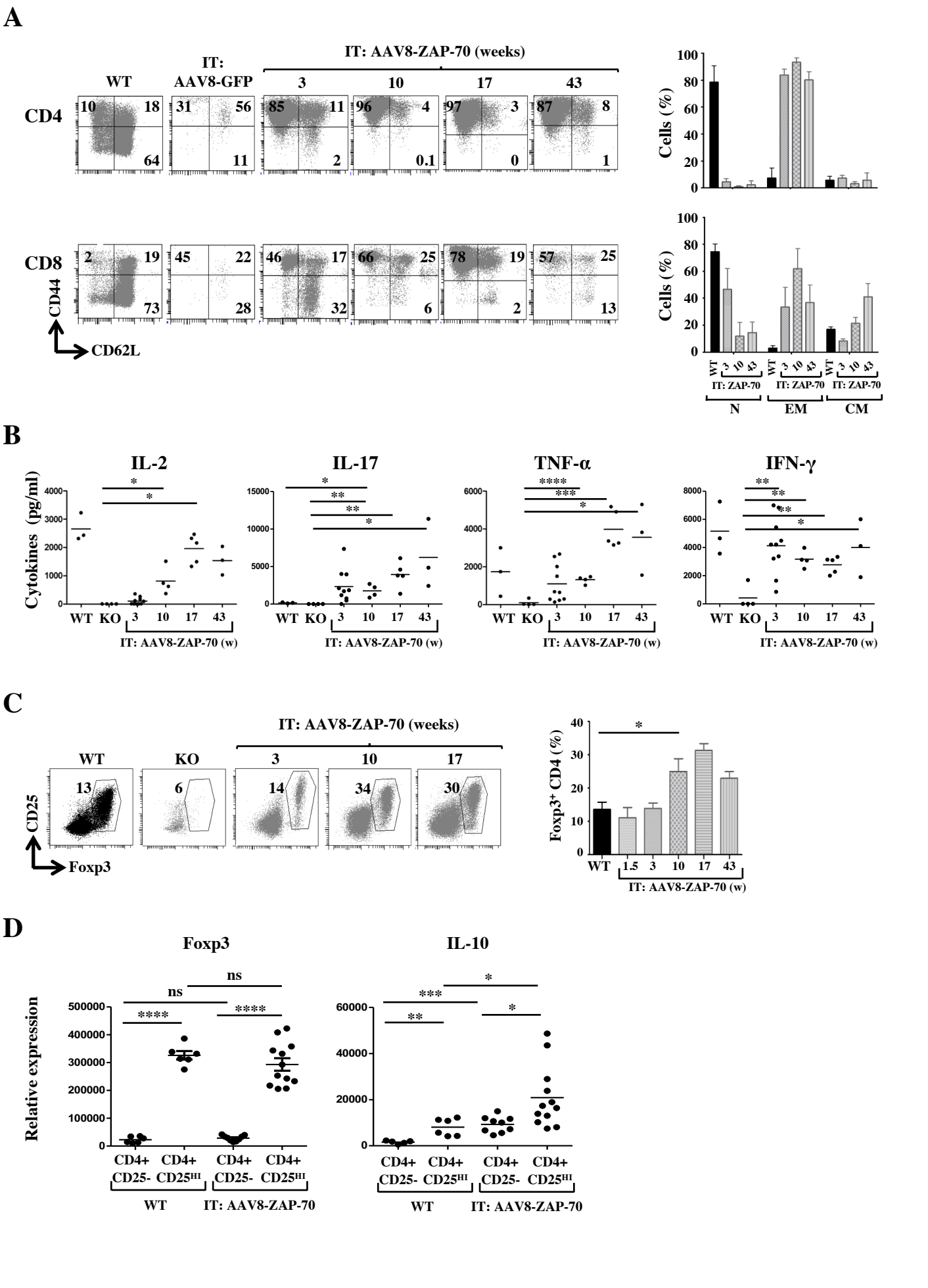
A
IT: AAV8-ZAP-70 (weeks)
WT
IT: AAV8-GFP
3
10
17
43
CD4
CD8
CD44
CD62L
Cells (%)
IT: ZAP-70
N
EM
CM
B
IL-2
IL-17
TNF-α
IFN-γ
Cytokines (pg/ml)
WT
KO
IT: AAV8-ZAP-70 (w)
C
IT: AAV8-ZAP-70 (weeks)
CD25
Foxp3
Foxp3+ CD4 (%)
1.5
IT: AAV8-ZAP-70 (w)
D
Foxp3
IL-10
Relative expression
CD4+ CD25-
CD4+ CD25HI
WT
IT: AAV8-ZAP-70

Fig E1

A

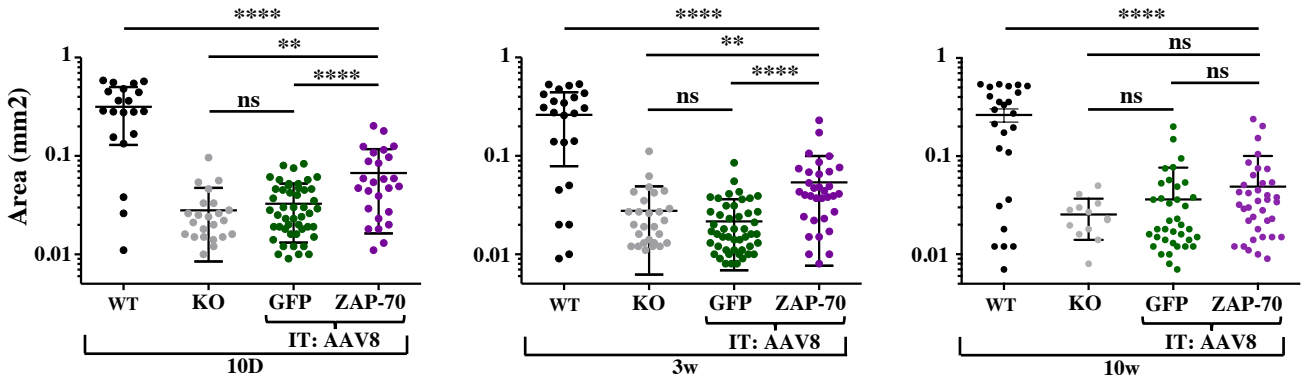
****
**
****
ns
1
0.1
0.01
Area (mm2)
WT
KO
GFP
ZAP-70
IT: AAV8
10D
3w
10w

B

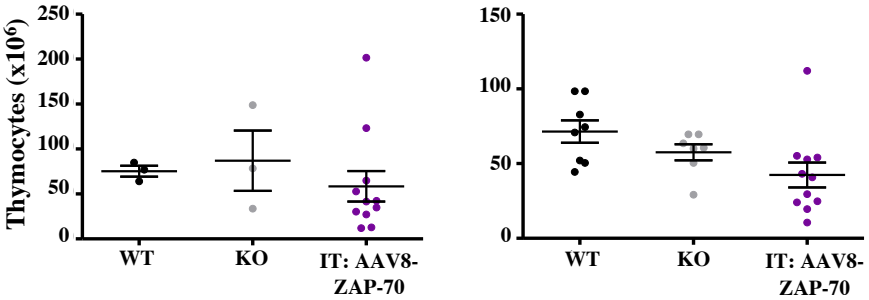
Thymocytes (x10⁶)
250
200
150
100
50
0
WT
KO
IT: AAV8-
ZAP-70

Fig E2

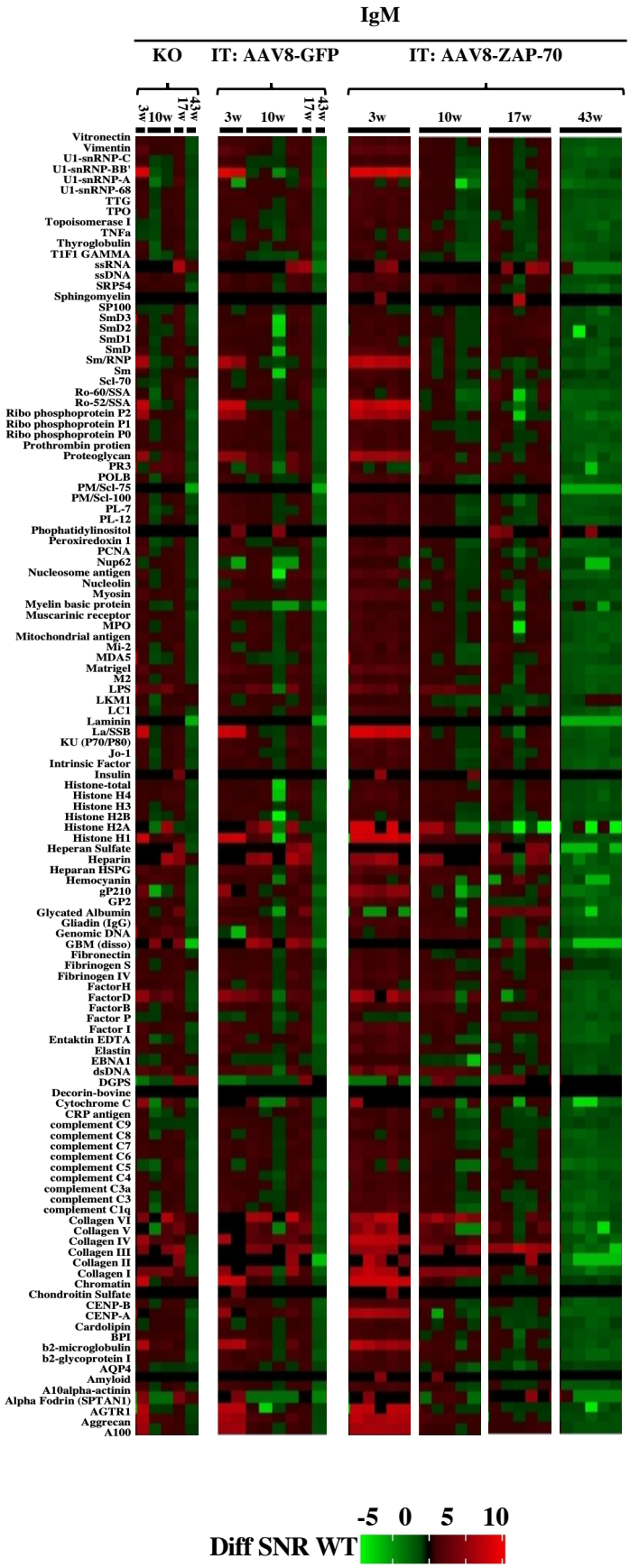
IgM
KO
IT: AAV8-GFP
IT: AAV8-ZAP-70
3w
10w
17w
43w
Vitronectin
Vimentin
U1-snRNP-C
U1-snRNP-BB'
U1-snRNP-A
U1-snRNP-68
TTG
TPO
Topoisomerase I
TNFa
Thyroglobulin
T1F1 GAMMA
ssRNA
ssDNA
SRP54
Sphingomyelin
SP100
SmD3
SmD2
SmD1
SmD
Sm/RNP
Sm
Scl-70
Ro-60/SSA
Ro-52/SSA
Ribo phosphoprotein P2
Ribo phosphoprotein P1
Ribo phosphoprotein P0
Prothrombin protien
Proteoglycan
PR3
POLB
PM/Scl-75
PM/Scl-100
PL-7
PL-12
Phophatidylinositol
Peroxiredoxin 1
PCNA
Nup62
Nucleosome antigen
Nucleolin
Myosin
Myelin basic protein
Muscarinic receptor
MPO
Mitochondrial antigen
Mi-2
MDA5
Matrigel
M2
LPS
LKM1
LC1
Laminin
La/SSB
KU (P70/P80)
Jo-1
Intrinsic Factor
Insulin
Histone-total
Histone H4
Histone H3
Histone H2B
Histone H2A
Histone H1
Heperan Sulfate
Heparin
Heparan HSPG
Hemocyanin
gP210
GP2
Glycated Albumin
Gliadin (IgG)
Genomic DNA
GBM (disso)
Fibronectin
Fibrinogen S
Fibrinogen IV
FactorH
FactorD
FactorB
Factor P
Factor I
Entaktin EDTA
Elastin
EBNA1
dsDNA
DGPS
Decorin-bovine
Cytochrome C
CRP antigen
complement C9
complement C8
complement C7
complement C6
complement C5
complement C4
complement C3a
complement C3
complement C1q
Collagen VI
Collagen V
Collagen IV
Collagen III
Collagen II
Collagen I
Chromatin
Chondroitin Sulfate
CENP-B
CENP-A
Cardolipin
BPI
b2-microglobulin
b2-glycoprotein I
AQP4
Amyloid
A10alpha-actinin
Alpha Fodrin (SPTAN1)
AGTR1
Aggrecan
A100
-5
0
5
10
Diff SNR WT

Fig E3

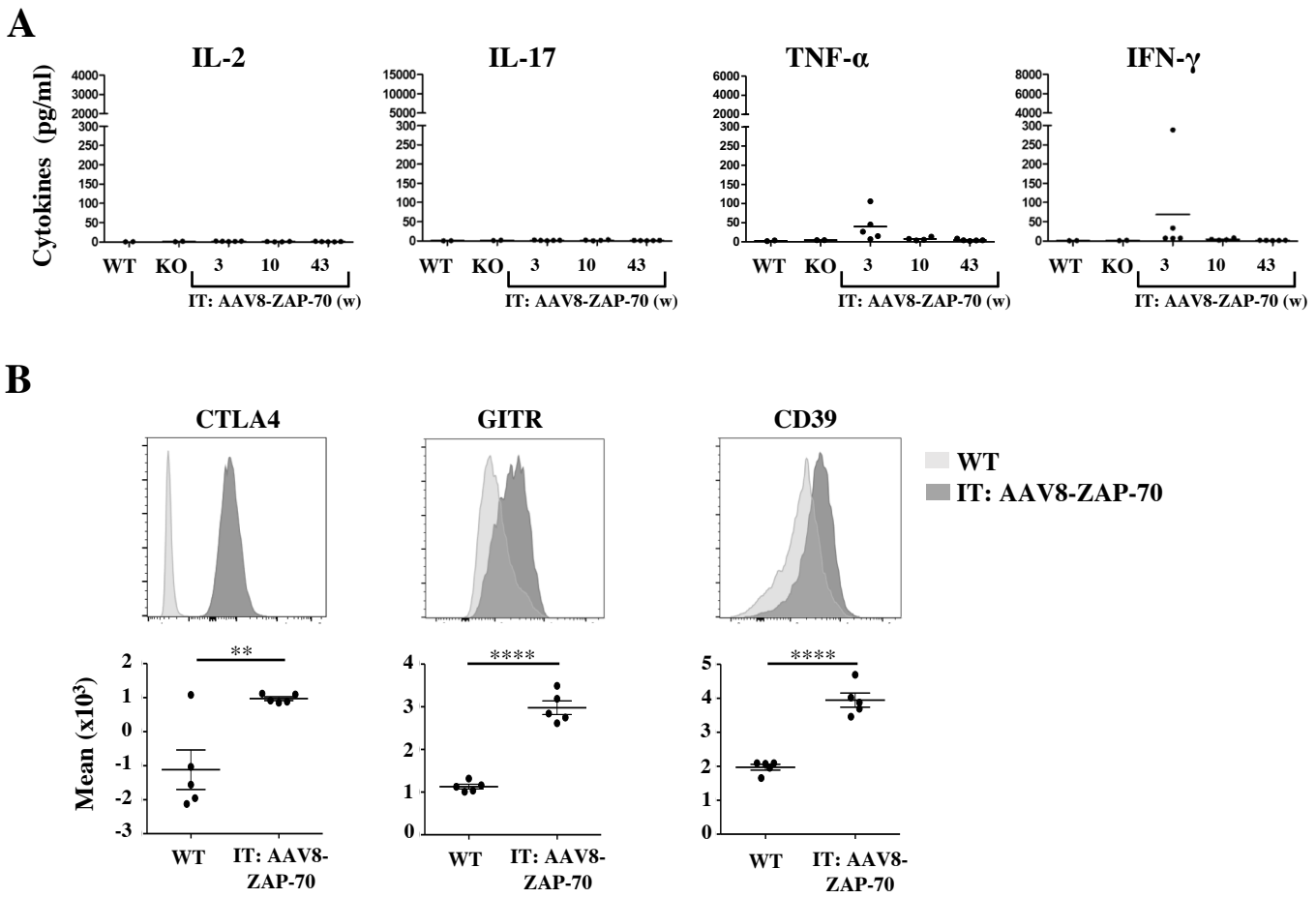
A
IL-2
IL-17
TNF-α
IFN-γ
Cytokines (pg/ml)
WT
KO
3
10
43
IT: AAV8-ZAP-70 (w)
B
CTLA4
GITR
CD39
WT
IT: AAV8-ZAP-70
Mean (x10³)
**
****
IT: AAV8-ZAP-70